Meereswissenschaftliche Berichte
MARINE SCIENCE REPORTS

No. 68

Redox Layer Model (ROLM): a tool for analysis of the water
column oxic/anoxic interface processes

by

Evgeniy V. Yakushev[1,2], Falk Pollehne[2], Günter Jost[2], Ivan Kuznetsov[1,2],
Bernd Schneider[2], Lars Umlauf[2]

**Institut für Ostseeforschung
Warnemünde
2006**

Addresses of authors:

[1]Shirshov Institute of Oceanology RAS, Southern Branch, Gelendzhik-7, Krasnodarski Kray, 353467, Russia
[2]Baltic Sea Research Institute (IOW), Seestraße 15, D-18119 Rostock-Warnemünde, Germany

Corresponding author: e_yakushev@yahoo.com

Yakushev, E.V.; Pollehne, F.; Jost G.; Kuznetsov I.; Schneider B.; Umlauf L.:

Redox Layer Model (ROLM): a tool for analysis of the water column oxic/anoxic interface processes

C o n t e n t s

Acknowledgements

4

1. Abstract

The goal of this coupled 1D hydrophysical-biogeochemical model was to study the cycling of main elements in the pelagic redox layer in Seas with anoxic conditions. The processes of formation and decay of organic matter (OM), reduction and oxidation of species of nitrogen, sulphur, manganese and iron, and transformation of phosphorus species were parameterized. The temporal and spatial development of the model variables were described by a system of horizontally integrated vertical diffusion equations for non-conservative substances. The calculated spatial and temporal distributions of parameters are in good agreement with observed vertical distribution patterns.

To study the influence of the seasonal variability on the chemical structure of the pelagic redox-layer in different system we used different hydrophysical scenarios of the Black Sea and the Baltic Sea. Results clearly showed that organic matter, formed during the bloom periods by phytoplankton, exerts a major direct influence on structure and processes in the remote redox-interface in both Seas. This is due to the competition for the dissolved oxygen between the oxidation of organic matter (particulate and dissolved) originating in the mixed layer and the oxidation of reductants supplied from the anoxic deep water. As a result of this competition, the processes of OM mineralization become more intense in summer, leading to increased activity of heterotrophic bacteria (both in oxic and anoxic zones), as well as of aerobic autotrophic bacteria (nitrifiers). The activity of the anaerobic chemolithotrophic organisms are reduced in summer, because less metal oxidants (which require oxygen for their formation) are available for reactions of anaerobic oxidation of sulfides and other reduced sulfur-species.

2. Introduction

Anoxic conditions in the water column are a natural feature of numerous areas in the world's seas. These conditions arise when transport rates of organic matter (OM) and oxygen into deeper layers are not balanced and oxygen is used up leaving an excess of organic material to be decomposed. The decomposition processes continue by bacterial activity employing other electron acceptors than oxygen and usually end up with reduction of sulphate (a major constituent in seawater). This last process leads to the production of hydrogen sulphide which is toxic to most higher life forms.

The energy derived from the oxidation of reduced inorganic compounds from the anoxic zone fuels the microbial community that produce OM via chemosynthesis (Nealson and Stahl, 1997; Sorokin, 2002; Canfield et al., 2005). These processes together with oxic, anoxic and suboxic OM mineralization and processes of chemical reactions between reduced and oxidized compounds are responsible for the complexity of the redox layer.

The mentioned imbalance between transport of OM and oxygen occurs when a hydrophysical structure with a well-pronounced pycnocline is created. The existence of such structures can be temporary or permanent, correspondingly creating zones of temporary or permanent anoxia (Fig. 1). The appearance of temporary water anoxia (as a consequence of eutrophication (Richardson and Jorgensen, 1996)) and changing volumes of permanent anoxic water bodies are a threat for the functioning of healthy aerobic ecosystems and thereby a direct danger to human health and economic welfare. Permanent anoxic conditions are observed in numerous lakes, fjords (for example, Framvaren), and also in some regions of the World Ocean (Black Sea, Baltic Sea Deeps, Cariaco Basin). The scales of processes that affect the formation of each system's hydrophysical structure vary from molecular diffusion to climatic variability. However, in lakes and fjords some processes, such as transport of water with geostrophic currents or mesoscale eddies, are unimportant, leading to less intense mixing than under marine conditions. Therefore, the chemical structure of redox interfaces in fjords and lakes are characterized by sudden changes in redox conditions and steep chemical gradients. In comparison to lakes and fjords, oxidation - reduction features at marine redox interfaces are characterized by gradual gradients, and gradually varying temporal changes as well. For example, the boundary of anoxic zone of the Cariaco Basin is influenced by mesoscale eddies that periodically supply dense water with high oxygen content to the anoxic zone (Scranton et al., 2006). Similarly, in certain years, mainly winter weather conditions in the Baltic Sea result in an influx of oxygen rich saline Northern Sea waters to the deep anoxic layers (Schneider et al., 2002; Feistel et al., 2003). The Black Sea oxic/anoxic interface appears to be more stable, because the Bosphorus Plume waters influences only the south-western part of the Black Sea.

The study of the processes responsible for the maintenance of redox interfaces should be optimally done with a combination of field measurements supplemented by modelling that allows jointly analysis of the complexity of processes studied by different scientific disciplines.

We describe here the modelling framework to be used in systems with anoxia observed in the water column. This 1D hydrophysical-ecological-biogeochemical O-N-S-P-Mn-Fe model allows us to simulate the main features of biogeochemical structure of the redox interfaces in the water columns of seas with anoxic conditions (i.e. vertical distributions of parameters, rates of processes). In this version of the model we consider the water column from the surface to about 100 m below the oxic/anoxic interface. In contrast to the previous versions of this model (Yakushev, 1992, 1999;

Yakushev and Neretin, 1997) we parameterize the processes of formation of organic matter during both photosynthesis and chemosynthesis and, therefore model a feedback between the upward fluxes of nutrients and the amount of produced OM.
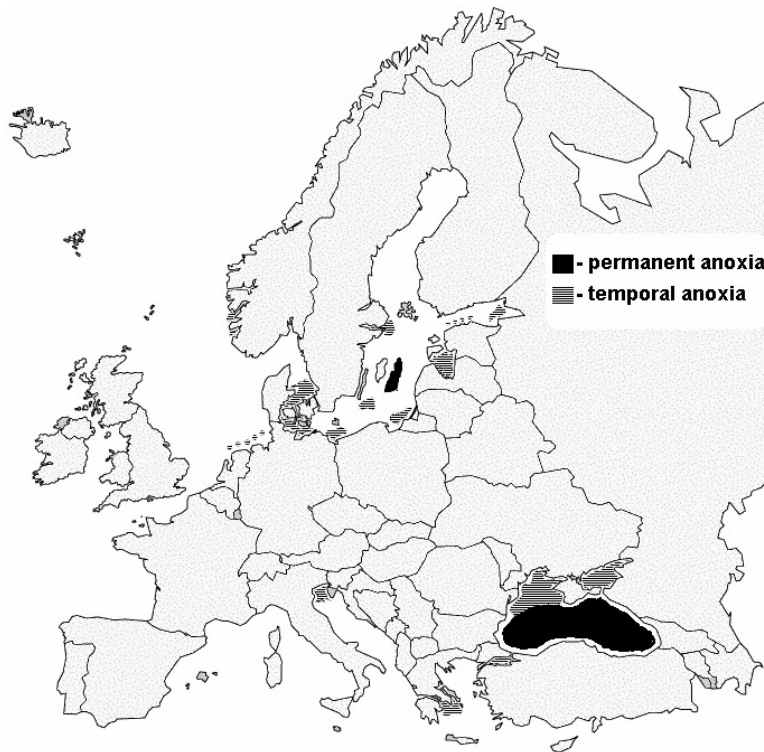
Fig. 1. Regions with permanent and temporal anoxia in the European Seas.

The goal of this work was to create an instrument for a complex analysis of the observing distributions of variables, processes controlling their interactions and for the analysis of changes in the biogeochemical structure of redox interfaces connected with variability in external factors.

In particular we will use this model for analysis of some key processes responsible for the formation of the redox layer structure, i.e. sulfide oxidation, oxygen consumption, formation of phosphate "dipole". We will also use this model for estimating whether the water column redox layers have seasonal variability in their structure and how this can be explained, We simulated the structure and seasonal behavior of a redox-interface with two hydrophysical "scenarios" – a simplified one for the Black Sea, and a more complicated one for the Baltic Sea, calculated with General Ocean Turbulent Model GOTM (Burchard et al., 1999).). Similarities of the results of different scenarios allowed us to obtain some numerical estimates that can reveal common features of the behavior of redox-interfaces.

3. Water column redox interfaces: Structure and processes

Redox interfaces of the different marine basins are characterized by a range of common features. The hydrochemical structure of the Black and the Baltic Sea oxic/anoxic interfaces are shown in Fig. 2. In both of these interfaces the nitrate maximum is observed at the depth where the vertical gradient of oxygen decreases (lower part of oxycline). The onset depths of increasing

concentrations of ammonia and dissolved manganese correspond to the position of the phosphate minimum (better seen in the Black Sea compared to the Baltic Sea). For the Black (Yakushev et al., 2002) and Baltic Seas this depth is identical with the depth of oxygen depletion. In both of these Seas, hydrogen sulphide appears 5-10 m deeper. All these features are related by the theoretical electron potential sequence of the oxidants and reductants (Canfield et al., 2005). The vertical distribution of transmission (Xmiss, Fig.2) is characterised by the presence of a turbidity layer in the vicinity of sulphide onset and of a layer of more transparent water above.
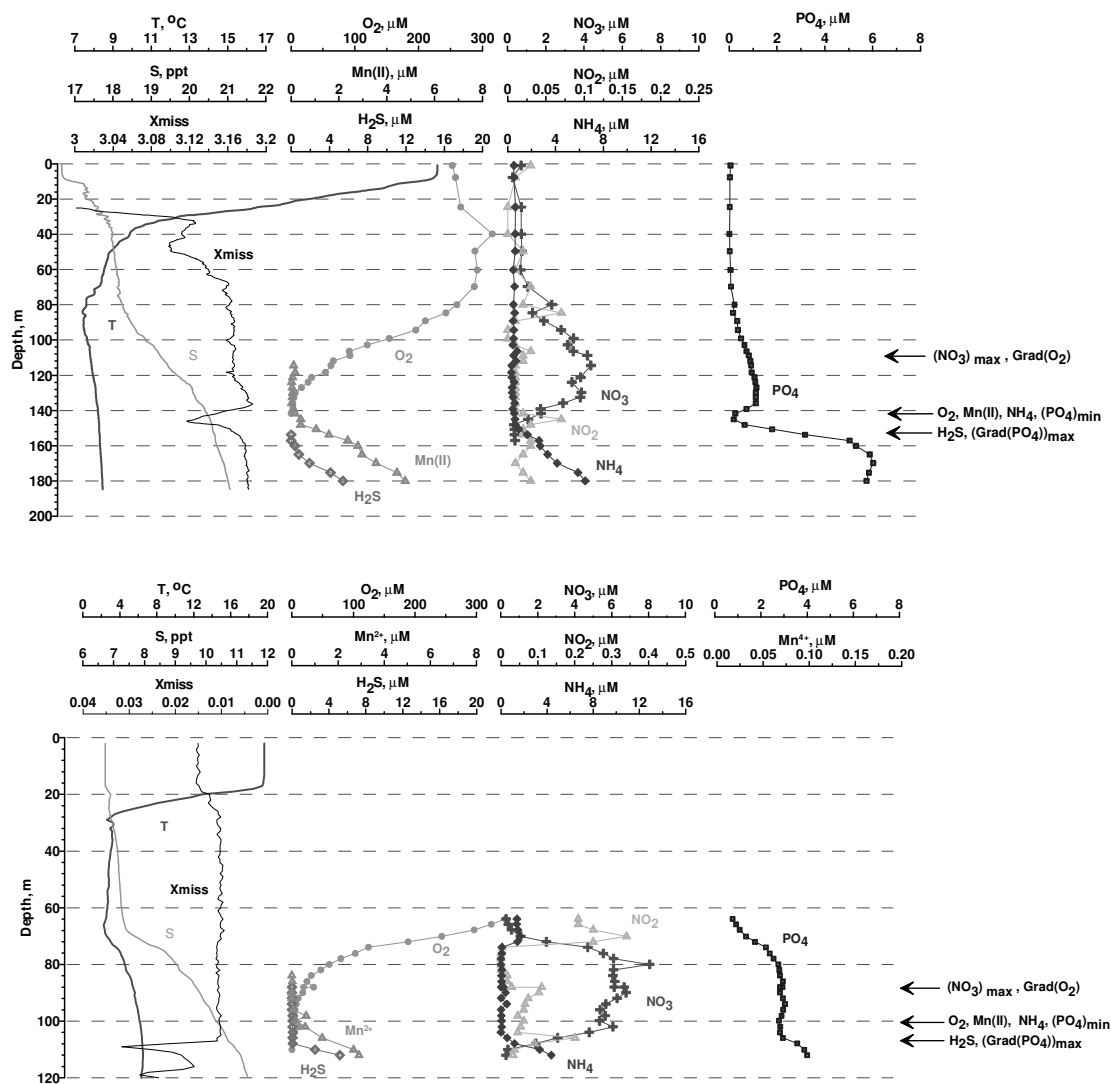
Fig. 2. Vertical distribution of hydrochemical parameters in the Black (upper panel) and Baltic (lower panel) Seas. The arrows shows the depths of (1) NO_3 maximum and lower part of oxycline (2) depletion of O_2, onsets of Mn(II) and NH_4, and PO_4 minimum, (3) onset of H_2S and maximum gradient of PO_4.

The Black Sea is probably the best location for study of redox-layer processes because of its stability. The Bosphorus only affects the southern-western region of the Sea. The central and peripheral Black Sea are characterized by stability of the chemical features (i.e. maximum positions, onset levels) in the density field (Vinogradov and Nalbandov, 1990; Murray et al., 1995).

Such a "chemotropicity" implies that there are no horizontal gradients of chemical variables along the same density surface, supporting the use of a 1D model for describing the processes responsible for the maintenance of the redox-layer chemical structure.

4. Methodology. Formulation of model

4.1 Main 1D model equation

The time-space evolution of the model variables is described by a system of horizontally integrated vertical diffusion equations for non-conservative substances:

$$\frac{\partial C_i}{\partial t} = \frac{\partial}{\partial z} K_z \frac{\partial C_i}{\partial z} - \frac{\partial ((W_C + W_{Mn})C_i)}{\partial z} + R_{Ci}$$

where C_i - concentration of a model variable; K_z - vertical turbulent diffusion coefficient; W_C is the sinking rate of particulate matter; W_{Mn}, - accelerated rate of sinking of particles with settling Mn hydroxides; $R_{Ci} = \sum_j Rate_{BjCi}$ - sources and sinks of a substance (rates of transformation) which is an algebraic sum if local fluxes are caused by biogeochemical interaction ($Rate_{BjCi}$).

The following variables (C_i) were considered in the model (Table 1.): Dissolved oxygen ($O2$), hydrogen sulfide ($H2S$), elemental sulfur ($S0$), thiosulfate ($S2O3$), sulfate ($SO4$), ammonia ($NH4$), nitrite ($NO2$), nitrate ($NO3$), particulate organic nitrogen (PON), dissolved organic nitrogen (DON), phosphate ($PO4$), particulate organic phosphorus (POP), dissolved organic phosphorus (DOP), bivalent manganese ($MnII$), trivalent manganese ($MnIII$), quadrivalent manganese ($MnIV$), bivalent iron ($FeII$), trivalent iron ($FeIII$), phytoplankton (Phy), zooplankton (Zoo), aerobic heterotrophic bacteria (B_ae_het), aerobic autotrophic bacteria (B_ae_aut), anaerobic heterotrophic bacteria (B_anae_het), and anaerobic autotrophic bacteria (B_anae_aut).

In the following description of the model we will use the names of variables assumed in the formulas of the model (i.e. "$NO3$" for NO$_3^-$, "$MnII$" for Mn(II) and "Phy" for phytoplankton, etc.).

Table 1. State variables of model. Concentrations are presented in micromoles for chemical variables and in wet weight (WW) for biological parameters.

Variable	Meaning	Dimension
O2	Dissolved Oxygen	μM O
S		
H2S	Hydrogen Sulfide	μM S
S0	Elemental Sulfur	μM S
S2O3	Thiosulfate	μM S
SO4	Sulfate	μM S
N		
NH4	Ammonia	μM N
NO2	Nitrite	μM N
NO3	Nitrate	μM N
PON	Particulate Organic Nitrogen	μM N
DON	Dissolved Organic Nitrogen	μM N
P		
PO4	Phosphate	μM P
POP	Particulate Organic Phosphorus	μM P
DOP	Dissolved Organic Phosphorus	μM P
Mn		
MnII	Bivalent Manganese	μM Mn
MnIII	Trivalent Manganese	μM Mn
MnIV	Quadrivalent Manganese	μM Mn
Fe		
FeII	Bivalent Iron	μM Fe
FeIII	Trivalent Iron	μM Fe
Biological patameters		
Phy	Phytoplankton	mgWW m^{-3}
Zoo	Zooplankton	mgWW m^{-3}
B_ae _het	Aerobic Heterotrophic Bacteria	mgWW m^{-3}
B_ae_aut	Aerobic Autotrophic Bacteria	mgWW m^{-3}
B_anae _het	Anaerobic Heterotrophic Bacteria	mgWW m^{-3}
B_anae_aut	Anaerobic Autotrophic Bacteria	mgWW m^{-3}

4.2 Hydrophysical Scenarios.

4.2.1 The Black Sea.

One dimensional models are very sensitive to values of K_z. The calculation of the K_z values in the redox-layer depth are usually made using the Gargett formula (Gargett, 1984), that takes into account the vertical density structure

$$K_z = a_0 N^{-q}, \text{ where } N = \sqrt{-\frac{g}{\rho}\frac{\partial \rho}{\partial z}}.$$

N- buoyancy frequency, g - acceleration of gravity, ρ- the mean density, a_0 and q - empirical coefficients;

Estimates for the Black Sea redox-layer obtained with the modification of Gargett formula

$$K_z = 1.62 \cdot 10^{-3} \cdot \left(\frac{g}{\rho} \frac{d\rho}{dz} \right)^{-0.5}$$ give the values about $1 \cdot 10^{-5}$ m^2 s^{-1} (Samodurov and Ivanov, 1998).

This formula was used for the redox-later features estimates by Konovalov et al. (2006). Smaller values ($5.2 \cdot 10^{-6}$ m^2 s^{-1}) were used for the Baltic Sea by Neretin et al. (2003)
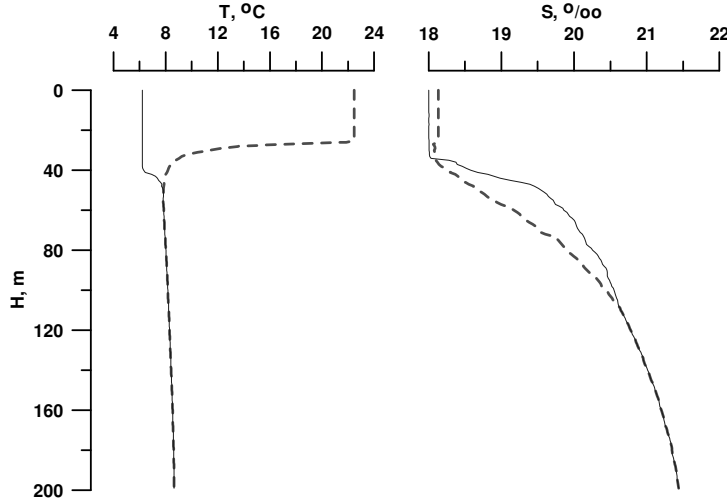
Fig. 3. Typical temperature and salinity distributions for the central Black Sea winter (solid) and summer (dotted). (Data from RV"Knorr" and RV "Akvanavt" cruises).

The estimates of K_z obtained by Stokozov (2004), who analyzed the spreading of ^{137}Cs after the Chernobyl accident, were about $1\text{-}3 \cdot 10^{-5}$ in the Black Sea Central Basin and $3\text{-}11 \cdot 10^{-5}$ m^2/s in the region of the rim current. These larger estimates, in our opinion should, be closer to the real values than calculations from the equation of Gargett, because they were calibrated with the flux of a real passive tracer and may reflect processes not considered in the above written formulas. Therefore values of vertical turbulent mixing coefficient for our model were re-calculated on the basis of the daily density vertical structure changes. For this we used the Gargett formula with empirical coefficients permitting values of K_z in the suboxic zone in the range of 10^{-5} -10^{-4} m^2 s^{-1}:

$$K_z = 1.94 \cdot 10^{-2} \cdot \left(\frac{g}{\rho} \frac{d\rho}{dz} \right)^{-0.5}$$

The results of these calculations are presented below.

The seasonal variability of light and hydrophysical structure were considered as external parameters. To describe the variability of the upper layer (from the surface to the cold intermediate layer), we considered the changes between two typical distribution observed at a station in the central part of the Black Sea in winter and summer (Fig. 3). It was assumed that the changes between the typical summer and typical winter structure occur according to a sinusoidal function. Daily calculated density values were used for estimating of the K_z values using the previously mentioned formula.

The changes of the photosynthesis rate as a function of light and temperature are described below.

4.2.2 The Baltic Sea.

For the Baltic Sea we used the results of calculation with the General Ocean Turbulence Model GOTM (Burchard et al., 1999) for 1992-1993, when the vertical distribution in the Gotland Basin was stable and a developed anoxia was observed. The calculated arrays of daily changes of T, K_Z and light were directly used in calculations.

4.3 Sinking.

The process of sinking of particulate matter is usually described as:

Sinking= $W_{Ci}.dC/dz$

where W_{Ci} is the rate of sinking. The values of W_{Ci} in the models were taken to be: for phytoplankton – 1 m d^{-1} (Savchuk and Wulff, 1996; Oguz et al., 1998), detritus – 1.5 m d^{-1} (Savchuk and Wulff, 1996), 5 m d^{-1} (Oguz et al., 1998), 3.5 m d^{-1} and 20 m d^{-1} (Gregoire et al., 1997). The Monod-type dependence was used in Oguz et al. (1998) to describe the changes of sinking depending on the concentrations of detritus.

In this model we also described the effect of increase of sinking rates when *MnIV* and *MnIII* oxides are formed. We analyzed this effect earlier (Yakushev and Debolskaya, 2000) and found that the precipitation of particulate Mn oxide can significantly increase the flux of this electron acceptor toward the sulfide boundary and that this increase in flux can affect the distribution of particles that may form a layer of more transparent water above the layer of increased turbidity. We parameterized this effect as follows:

$$W_{Ci}=W_{Ci}+W_{Me}*MnIV/(MnIV+0.1)$$

where: W_{Ci} is a rate of sinking. We assumed $W_{PON} = W_{POP} = 6.0$ m d^{-1}, $W_{Phy} = 0.5$ m d^{-1}, $W_{Zoo} = 1.0$ m d^{-1}, and $W_{Bact\,I} = 0.5$ m d^{-1} for all the bacteria. $W_{Me} = 16$ m d^{-1} was taken to be the sinking rate of manganese and iron oxides.

4.4 Boundary conditions

A 1D water column was considered which ranged between the sea surface (upper boundary) and a water depth of 200 m (lower boundary).

4.4.1 Upper Boundry:

Except for O_2, PO_4 and inorganic nitrogen compounds, the surface fluxes of other chemical constituents considered in the model were assumed to be zero. The O_2 exchange is given by the flux equation:

$Q_{O2} = k_{660} * (Sc/660)^{-0.5} * (Oxsat-O2)$

with:
Oxsat –oxygen saturation concentration as a function of temperature and salinity according to UNESCO (1986);

Sc – Schmidt number (the ratio between the kinematic viscosity and the diffusion coefficient), calculated according to Wanninkhof (1992);

k_{660} – reference (Sc = 660, CO_2 at 20°C) gas exchange transfer velocity;

A variety of different empirical functions have been proposed to describe k_{660} as a function of wind speed. Here we used a relationship that was obtained from CO_2 flux measurements in the Baltic Sea (Weiss et al., 2006):

$k_{660} = 0.365 * u^2 + 0.46 * u$

(wind u in m s^{-1} gives k_{660} in cm h^{-1})

The model simulations were performed with a mean wind speed of 5 m/sec.

Fonselius (1974) found on the basis of his model of the phosphorus balance in the Black Sea that about 6700 tons/year must be added to the Black Sea sediments. Therefore the input of phosphorus with the rivers and the atmospheric precipitates must be significant.

Because this model consider a seasonal timescale, it was necessary to parameterize the flux of the nutrients connected with the riverine input and with atmospheric deposition:

For the Black Sea we accepted:
Q_{PO4} = 0.13 mmol m^{-2} d^{-1} for PO_4, Q_{NO3} = 1.5 mmol m^{-2} d^{-1} for NO_3

For the Baltic Sea:
Q_{PO4} = 0.0085 mmol m^{-2} d^{-1} for PO_4, Q_{NO3} = 0.46 mmol m^{-2} d^{-1} for NO_3 (calculated on the basis of estimates of Total-N (990000 t/year) and Total-P (40000 t/year) for 415266 km^2 (HELCOM, 2002)

4.4.2 Lower Boundary:

Because this model doesn't consider variability below 200 m we assumed constant values of the main reductant concentrations at the lower boundary. In accordance to the observations, the following values were assumed: for the Black Sea: *NH4* = 20 μM, *H2S* = 60 μM, *MnII* = 8 μM, *FeII* = 0.4 μM, *PO4* =4.5 μM, for the Baltic Sea: *NH4* = 10 μM, *H2S* = 40 μM, *MnII* = 10 μM, *FeII* = 0.4 μM, *PO4* = 4.5 μM. For the other parameters we assumed the condition of the absences of flux.

4.5 Parameterization of the biogeochemical processes.
4.5.1 General remarks.

For the formal description of the chemical and biological pathways (shown in Fig. 4), we used our own parameterizations (Yakushev, 1992, 1999; Yakushev and Mikhailovskiy, 1996; Yakushev and Neretin, 1997) as well as that of others (Fasham et al., 1990; Fennel and Neuman, 2004; Ayzatullin and Leonov, 1975; Savchuk and Wulfff, 1996; Boudreau, 1996; Oguz et al, 1998; Gregoire et al., 1997; Konovalov et al., 2006). The values of the coefficients necessary for the rates descriptions were obtained from literature or from fitting model to measured concentrations profiles.

In general, the parameterization of rates of the biogeochemical interactions, Rate$_{BG,}$ were as follows:

$Rate_{BG} = K_{BG}\ Dep_{re1}\ Dep_{re2}\ [Dep_{inh}]$
K_{BG} – a constant
Dep_{re1}– dependence on concentration of the 1st reacting variable;
Dep_{re2}– dependence on concentration of the 2st reacting variable;
Dep_{inh} - dependence on concentration of a variable that inhibits the reaction.

When possible we used the simplest linear dependence (such as first order kinetics). This assumption is appropriate for for reactions of substances that coexist only in small concentrations as *O2* and *H2S* or *NO3* and *FeII*. We used non-linear dependence (i.e. Michaelis-Menten) in situations when the concentrations of the considered substances differed significantly or were mediated by bacteria (for instance description of a switch between oxic OM decay and denitrification). A function of inhibition was added as an additional switch to describe, for instance, the possibility of reactions in anoxic conditions.

These *Rate$_{BG}$* were parameterized for specific processes as follows:
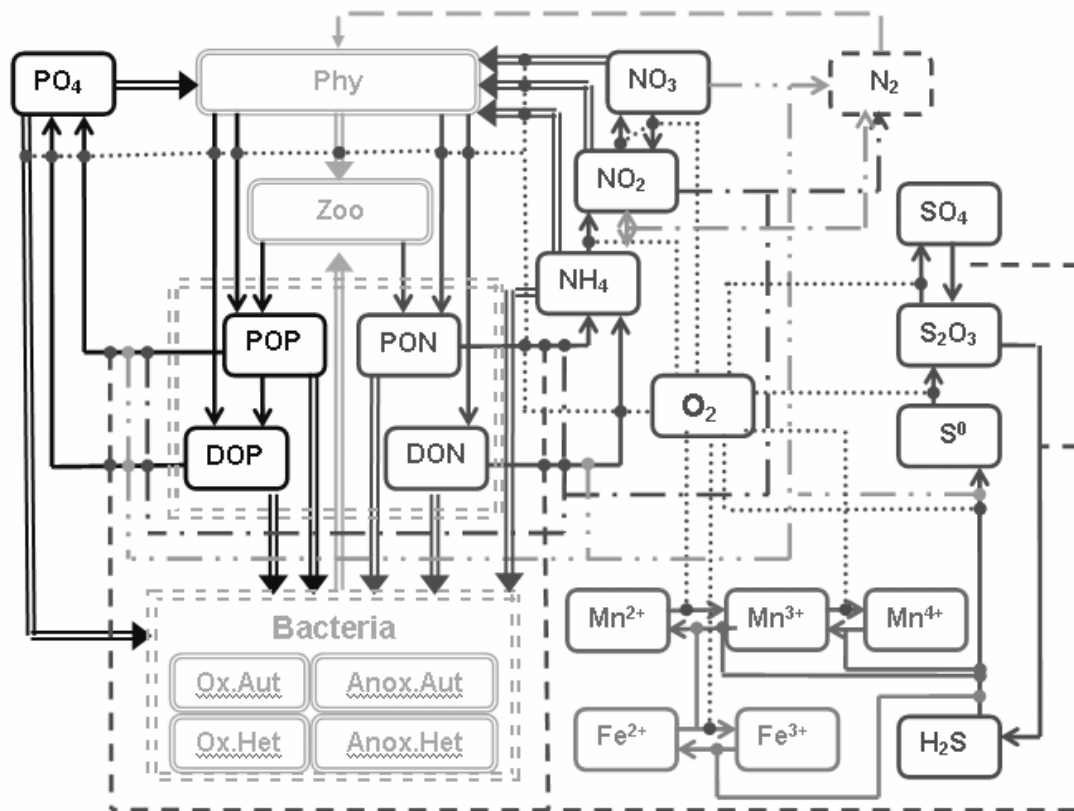

Fig. 4. Flow-chart of biogeochemical processes in the model.

4.5.2 Autolysis

The processes of decomposition of particulate to dissolved organic matter are usually described with a first order equation with a constant coefficient. Typical values for the coefficient are 0.10 d^{-1} (Oguz et al., 1998) or 0.004-0.18 d^{-1} (Gregoire et al., 1997). We assumed the following:

AutolisP = K$_{PD}$*POP

Where K_{PD} = 0.10 d^{-1}

4.5.3 Mineralization of OM

Mineralization of OM is a key process for modeling of formation of the oxygen-deficient and anoxic conditions, because the electron acceptor of this reaction changes from oxygen to nitrate (in case of depletion of oxygen). In the case of depletion of both oxygen and nitrate, metal oxides and sulfate can be used. The rates of mineralization with different electron acceptors are different (Canfield et al., 2005). Formation of OM from CO_2 (Methanogenesis) or fermentation of organic matter to methane and CO_2 should not be significant in sea water, because of the large amount of sulfate. The microbial degradation of different groups of OM with different labilities differs over time scales ranging from hours to millions of years. (Canfield et al., 2005). The detailed kinetics of the decomposition (needed for modeling long-term processes, for instance in the sediments) can be described with so-called 'multi-G' models with OM divided into several compartments with different particular degradability (Boudreau, 1996).

In this model we used a simplified approach. The OM was divided into DOM and POM with different rates of mineralization with different electron acceptors. We considerer POM as a detrital labile OM that can be "mineralized directly" with instantaneous autolysis. Such an approach is widely used in the models when it is necessary to describe the processes of mineralization and sedimentation of the same matter. We used the stoichiometry of the mineralization reactions presented by Richards (1965), and assumed the stoichiometric ratios to be the same in OM in oxic and anoxic conditions.

4.5.4 Mineralization in oxic conditions

$(CH_2O)_{106}(NH_3)_{16}H_3PO_4 + 106O_2 = 106CO_2 + 16NH_3 + H_3PO_4 + 106H_2O$
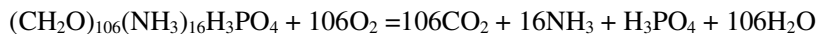
It is usually assumed that the processes of release of phosphate (phosphatification) and release of ammonia (ammonification) are parallel and occur with the same rate. Ammonification is carried out by heterotrophic bacteria that use amino acids and proteins as a source of nitrogen, leading to appearance of ammonia as the final product of mineralization. Phosphatification is also carried out by heterotrophs (Canfield et al., 2005).

The rate of this process is described as a first order equation, with the rate dependent on the amount of organic matter.

DcOM_O2= K$_{ND4}$*OM

Where *OM* – concentration of organic matter, K_{ND4}- constant with values 0.1-1 d^{-1} (Ward, Kilpatrick, 1991). The rates of phosphate and ammonia release have been assumed to be equaled in models (Yakushev and Mikhailovskiy, 1995; Fennel and Neumann, 2004).

The dependence of ammonification on temperature can be described by addition of an multiplier: *exp(0.15 t)* (Savchuk and Wulff, 1996; Fennel and Neumann, 2004) with corresponding change of K_{ND4} values (0.002 d^{-1} in Savchuk and Wulff, 1996). Concentrations of O_2 significantly affect the rates of oxygen consumption (Canfield et al., 2005), and in some models (Konovalov et al., 2006) the nonlinear dependence on oxygen is described by a multiplier: $O_2^{0.5}$.

In our version of the model we parameterized the dependence of decomposition of organic matter (for *DON* and *PON*) in oxic conditions as follows:

DcDM_O2=exp(Ktox*t)*K$_{ND4}$*DON*Fox
DcPM_O2=exp(Ktox*t)*K$_{NP4}$*PON*Fox

Thus we included the influences of temperature (as mentioned above) and Michaelis-Menten dependence on concentrations on dissolved oxygen.

$$Fox= \begin{cases} =0 & \text{for } O2 \leq O2ox \\ \\ =(O2-O2ox)/(O2-O2ox+Kox) & \text{for } O2 > O2ox \end{cases}$$

Where the following are taken as the indicated constants:
Kox = 15 μM is the half saturation constant for oxic mineralization,
O2ox = 0 μM is the oxygen parameter for oxic mineralization,
Ktox=0.15 $^{o}C^{-1}$ is the temperature parameter for oxic mineralization,
K_{ND4}= 0.01 d^{-1} is the specific rate of decomposition of *DON,*
K_{NP4}= 0.04 d^{-1} is the specific rate of decomposition of *PON,*

4.5.5 Mineralization in suboxic conditions

In suboxic conditions OM mineralization can occur with oxidized compounds of nitrogen, manganese and iron. The concentrations of iron in the water are very low and the contribution of total Mn reduction to carbon oxidation is small, <10% of total benthic mineralizaion (Thamdrup, 2000), thus we don't concider these processes in the model. The most significant process is denitrification. Denitrification is carried out by heterotrophic bacteria under low concentrations of oxygen if there is availability of oxidized nitrogen compounds (mainly NO_3 and NO_2).

$(CH_2O)_{106}(NH_3)_{16}H_3PO_4 + 84.8HNO_3 = 106CO_2 + 42.4N_2 + 148.4H_2O + 16NH_3 + H_3PO_4$

The relative consumption of NO_3 and NO_2 in the classic reaction (Richards, 1965) can be calculated in accordance to Anderson et al. (1982):

$1/2CH_2O + NO_3^- \rightarrow NO_2^- + 1/2H_2O + 1/2CO_2$
$3/4CH_2O + H^+ + NO_2^- \rightarrow 1/2N_2 + 5/4H_2O + 3/4CO_2$
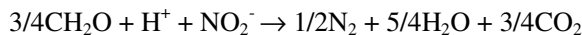
According to observations, denitrification and nitrification have both been observed at $O_2 < 60$ μM in a fjord (Zopfi et al., 2001), but the transition from nitrification to nitrate reduction occurs when

oxygen content decreases in various oxygen-deficient ecosystems below 0.9-6.3 µM (Lipschultz et al., 1990). The influence of oxygen on the rate of denitrification is usually described with a hyperbolic function (Savchuck and Wulfff, 1996; Fennel and Neumann, 2004). Rates of denitrification in cultures follow Michaelis-Menten kinetic with average half saturation constant of 50 µM NO3 (Canfield et al., 2005).

In this model we considered denitrification of particulate (*Denitr1_PM*, *Denitr2_PM*) and dissolved (*Denitr1_DM*, *Denitr2_DM*) organic matter carrying out in two stages: with NO_3 and NO_2, correspondingly:

*Denitr1_PM=K$_{N32}$*Fdnox* FdnNO3*PON*
Denitr2_PM=K$_{N24}$ Fdnox * FdnNO2*PON*
Denitr1_DM=K$_{N32}$ Fdnox * FdnNO3*DON*
Denitr2_DM=K$_{N24}$ Fdnox * FdnNO2*DON*

where
K_{N32} = 0.12 d^{-1} is the specific rate for 1st stage of denitrification,
K_{N24} = 0.20 d^{-1} is the specific rate for 2d stage of denitrification,
Fdnox – dependence on *O2*.

$$Fdnox= \begin{cases} =0 & \text{for } O2>O2dn \\ =1 - O2/(O2dn*(O2dn+1-O2)) & \text{for } O2 \leq O2dn \end{cases}$$

where *O2dn*=25 µM is the oxygen parameter for denitrification.

FdnNO3, FdnNO2 are the dependences of rates on concentrations of *NO3* and *NO2* respectively

$$FdnNO3= \begin{cases} =0 & \text{for } NO3 \leq NO3mi \\ = (NO3-NO3mi)/(NO3-NO3mi+1.) & \text{for } NO3 > NO3mi \end{cases}$$

$$Fdnox= \begin{cases} =0 & \text{for } NO2 \leq NO2mi \\ (NO2-NO2mi)/(NO2-NO2mi+0.02) & \text{for } NO2 > NO2mi \end{cases}$$

where
NO3mi= $1 \cdot 10^{-3}$ µM is the *NO3* parameter for denitrification,
NO2mi=$1 \cdot 10^{-4}$ µM is the *NO2* parameter for denitrification.

We have ignored the influence of temperature because denitrification takes place in layers with little significant seasonal temperature changes.

4.5.6 Sulfate reduction

$(CH_2O)_{106}(NH_3)_{16}H_3PO_4 + 53SO_4^{2-} = 106CO_2 + 106H_2O + 16NH_3 + H_3PO_4 + 53S^{2-}$

The process of sulfate reduction begins when oxygen and nitrate are exhausted. Sulfate reduction in the model occurs at an oxygen concentration of < 5 µM according to Cariaco Basin data (Yakushev and Neretin, 1997), where the upper threshold of active sulfate reducing bacteria occurs at 5 µM.

In this model we considered 2 stages of this processes that involve reaction with sulfate and thiosulfate.

$s4\_rd\_PM=K\_s4\_rd*$ Fsox Fsnx SO4*PON
$s4\_rd\_DM=K\_s4\_rd*$ Fsox Fsnx SO4*DON
$s23\_rd\_PM=K\_s23\_rd*$ Fsox Fsnx PON*S2O3
$s23\_rd\_DM= K\_s23\_rd*$ Fsox Fsnx DON*S2O3

where
$K\_s4\_rd = 2.5 \cdot 10^{-7}$ d^{-1} is the specific rate of sulfate reduction with sulfate,
$K\_s23\_rd =1.2$ d^{-1} is the specific rate of sulfate reduction with thiosulfate.

We used "hard switches" for *Fsox and Fsnx:*

$$Fsox= \begin{cases} =0 & \text{for } O2>O2sr \\ =1 & \text{for } O2\leq O2sr \end{cases}$$

$$Fsnx= \begin{cases} =0 & \text{for } NO3+NO2>NOsr \\ =1 & \text{for } NO3+NO2\leq NOsr \end{cases}$$

where *O2sr*= 25 µM is the oxygen parameter for sulfate reduction, *NOsr*=0.5 µM is the *NO3* and *NO2* parameter for sulfate reduction.

According to the stoichiometry of reaction with sulfate reduction, the decay of organic matter (in N units) was estimated as:

$DcPM\_SO4=16./53.*(s4\_rd\_PM+s23\_rd\_PM)$
$DcDM\_SO4=16./53.*(s4\_rd\_DM+s23\_rd\_DM)$

4.5.7 Ammonification and release of phosphate (phosphatification)

The total ammonification of *PON* and *DON* was calculated as:

$AmmonPON=DcPM\_O2+DcPM\_NO3+DcPM\_SO4$
$AmmonDON=DcDM\_O2+DcDM\_NO3+DcDM\_SO4$

The Redfield stoichiometry was used to estimate the phosphatification:

$PhosPOP=AmmonPON/16.$
$PhosDOP=AmmonDON/16.$

4.5.8 Nitrification

Nitrification, the oxidation of *NH4* to *NO3*, occurs in several stages and is accomplished mainly by chemolithotrophic bacteria (Canfield et al., 2005):

$NH_4^+ + 1.5\ O_2 \rightarrow NO_2^- + 2H^+ + H_2O$;
$NO_2^- + 0.5\ O_2 \rightarrow NO_3^-$;
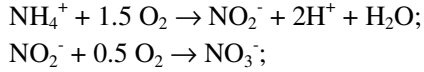
Estimates of the lowest oxygen threshold of nitrification vary from 0.4-0.9 to 3.1-4.9 μM (Lipschultz et al., 1990).

The kinetic function for nitrification can be described as a first order reaction for the oxic waters, but in the models for low oxygen content an approach is used where the rate of this process depends on the content of both oxygen and ammonia (Savchuk and Wulff, 1996). It can be described using multiplication of concentrations of oxygen and ammonia or multiplication of the results from the Michaelis-Menten hyperbolic formulas (Savchuk and Wulff, 1996).

We used the following functions for parameterization of nitrification in 2 stages:

Nitrif1=K_{N42}*NH4*O2/(O2+O2nf)
Nitrif2=K_{N23}*NO2*O2/(O2+ O2nf)

K_{N42}= 0.9 d^{-1} is the specific rate of the 1st stage of nitrification,
K_{N23} = 2.5 d^{-1} is the specific rate of the 2d stage of nitrification
These rate constants are maximum rates of 1st and 2d stages of nitrification.

O2nf=1 μM – is the oxygen parameter for nitrification.

4.5.9 Nitrogen fixation

The nitrogen fixation process is accomplished by several species of cyanobacteria that develop in the conditions of presence of phosphate and absence of available fixed nitrogen. In this model we used the formulation introduced by Savchuk and Wulff (1996) applying a limiting nutrient criterion based on the N/P ratio:

$$Nfixation = K_{Nfix}^{max} \frac{1}{1+\left(\dfrac{NO3+NO2+NH4}{16PO4}\right)^4} \frac{PO4}{PO4+0.3} Phy \cdot K_{NF} \cdot LimLight \cdot LimT \cdot Sn$$

where $K_{Nfix}^{max} = 20$ d^{-1} is the specific rate of nitrogen fixation. The latter symbols are explained below. In the frame of this model the nitrogen fixation results in increase of ammonia.

4.5.10 Anammox

The process of anoxic ammonia oxidation (anammox) (the reaction between nitrite and ammonia)

$NO_2 + NH_4 \rightarrow N_2 + 2H_2O$
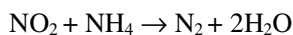
was found in the marine environment only recently (Dalsgaard et al., 2003, Kuypers et al., 2003). It is supposed that this reaction is mediated by chemolithotrophic bacteria (Canfield et al., 2005). This reaction requires a constant source of nitrite that can be provided either from reduction of *NO3* or oxidation of *NH4* (Murray, Yakushev, 2006).

We parameterized this process with a second order equation:

Anammox= NO2*NH4*K$_{annamox}$

with specific rate of anammox *K$_{annamox}$* =0.03 d^{-1}.

4.5.11 Oxidation of reduced sulfur forms with oxygen

We considered 3 stages of oxidation of *H2S* with *O2* (where *S2O3* are *S0* are intermediate forms) (Volkov, 1974).

$$2H_2S + O_2 \rightarrow 2S^0 + 2H_2O;$$
$$2S^0 + O_2 + H_2O \rightarrow S_2O_3^{2-} + 2H^+;$$
$$S_2O_3^{2-} + 2O_2 + 2OH^- \rightarrow 2SO_4^{2-} + H_2O;$$
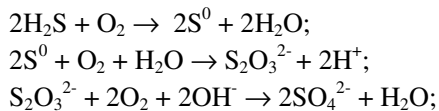
and parameterized these processes as follows:

hs_ox=K$_{\_hs\_ox}$*H2S*O2
s0_ox=K$_{\_s0\_ox}$*S0*O2
s23_ox=K$_{\_s23\_ox}$*S2O3*O2

where *K$_{\_hs\_ox}$* =0.2 d^{-1} is the specific rate of oxidation of *H2S* with *O2*,
K$_{\_s0\_ox}$ = 4.0 d^{-1} is the specific rate of oxidation of *S0* with *O2*,
K$_{\_s23\_ox}$ = 1.5 d^{-1} is the specific rate of oxidation of *S2O3* with *O2*.

4.5.12 S^0 - disproportionation

We considered the S^0 disproportionation in accordance to Canfield et al. (2005):

$$4S^0 + 3H_2O \rightarrow 2H_2S + S_2O_3^{2-} + 2H^+$$
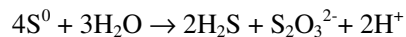
This process is assumed to be connected with autotrophic bacteria.

Disprop = Kdisp*S0

where *Kdisp* = 0.01 d^{-1} is the specific rate of S^0 disproportionation.

4.5.13 Thiodenitrification (chemolithotrophic denitrification)

Thiodenitrification, a process of oxidation of sulfide with nitrate and nitrite is carried out by autotrophic bacteria (Canfield et al., 2005).

$$3H_2S + 4NO_3^- + 6OH^- \rightarrow 3SO_4^{2-} + 2N_2 + 6H_2O$$
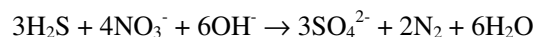
We considered it to be independent of the oxygen content:

sulfido=K_T *H2S*NO3
sulfido2= K_{T*}H2S*NO2,

where K_T= 0.8 μM^{-1}d^{-1} is the specific rate of thidenitrification.

4.5.14 Processes of oxidation and reduction of manganese and iron

The cycles of iron and manganese at the redox interface are similar. Both metals are present under anoxic conditions in dissolved reduced forms Mn(II) and Fe(II). Under oxic conditions they are oxidized by oxygen (Fe(II) also can be oxidized by nitrate or Mn(IV)) with formation of particulate hydroxides (MnO_2 and FeOOH).

These hydroxides sink and are reduced under anoxic conditions with sulfides, OM and ammonia (iron only). Recent studies revealed that both reduction and oxidation of Mn occur with Mn(III) as an intermediate form (Kostka et al., 1995; Webb et al., 2005, Trowborst et al., 2006).

4.5.15 Manganese (II) oxidation with oxygen:

It is usually assumed that bacterially-mediated Mn oxidation is the only process of Mn oxidation in natural waters (Tebo, 1991; Neretin et al., 2003). This rate of this process depends on concentrations of both Mn(II) and O_2 (Richardson et al., 1988).

The rate of the oxidation reaction of reduced manganese and oxygen

$$Mn^{2+} + 0.5\ O_2 + 2\ OH_. \rightarrow MnO_2 + H_2O$$
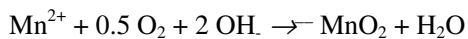
was parameterized as:

mn_ox=K_{_mn_ox}*Mn2*O2

where $K_{\_mn\_ox}$=1 d^{-1} is the *MnII* oxidation with *O2* constant.

4.5.16 Manganese (IV) reduction with sulfide

$$MnO_2 + HS^- + 3H^+ \rightarrow S^o + Mn^{2+} + 2H_2O$$
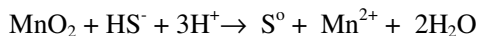
The kinetic of this process is very fast with half time on the order of seconds or minutes (Yao and Millero 1996; Neretin et al., 2003). This process can occur chemically (Canfield et al., 2005; Nealson et al., 1991) and can be accomplished by autotrophs. The experimental study of Mn(IV) reduction by bacteria *Schewanella Putrefaciens* (Dollhopf et al., 2000) revealed that this processes maximum rate can reach 0.04 min^{-1} (about 60 d^{-1}). This processes rate is inhibited by nitrate.

It was parameterized as:

mn_rd=K_{_mn_rd}*MnIV*H2S

where $K_{\_mn\_rd}$=4 d^{-1} is the *MnIV* reduction with sulfide constant.

4.5.17 Manganese (III) oxidation and reduction

Recently, production of dissolved, oxidized Mn in the form of Mn(III) by Mn(II)-oxidizing bacteria and in incubations with Black Sea suboxic zone water has been observed (Webb et al., 2005). Dissolved Mn(III) has also been directly observed in the suboxic zone (Trouwborst et al., 2006). Mn(III) is an important intermediate product of the Mn cycle and can exist in both dissolved and solid forms (Kostka et al., 1995).

The stoichiometry of the reactions of Mn(III) oxidation process can be Canfield et al. (2005):

$$4Mn^{2+} + O_2 + 4H^+ \rightarrow 4Mn^{3+} + 2H_2O$$
$$4Mn^{3+} + O_2 + 6OH^- \rightarrow 4MnO2 + 6H2O$$
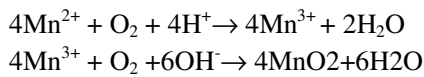
Mn(III) can be also produced as an intermediate during the Mn(IV) reduction (Ali and Ahiq, 2004; Kostka et al., 1995):

$$2MnO_2 + 7H^+ + HS^- \rightarrow 2Mn^{3+} + 4H_2O$$
$$2Mn^{3+} + HS^- \rightarrow 2Mn^{2+} + S^0 + H^+$$
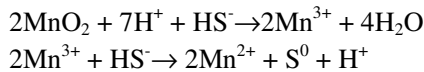
Mn(III) can be complexed with organic and inorganic ligands (Webb et al., 2005) and also can form insoluble hydroxides (Canfield et al., 2005):

$$Mn^{3+} + 2H_2O \rightarrow MnOOH + 3H^+$$
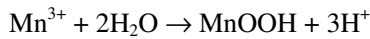
In the latest variants of the model we added these processes connected with Mn(III) formation and removal due to both reduction and oxidation of Mn. We parameterized them as follows:

mn_ox=$K_{\_mn\_ox}$*O2*MnII
mn_ox2=$K_{\_mn\_ox2}$*O2*MnIII
mn_rd=$K_{\_mn\_rd}$*MnIV*H2S
mn_rd2=$K_{\_mn\_rd2}$*MnIII*H2S

where $K_{\_mn\_ox}$ = 0.5 d^{-1} is the *MnII* oxidation with *O2* constant,
$K_{\_mn\_ox2}$ = 15 d^{-1} is the *MnIII* oxidation with *O2* constant,
$K_{\_mn\_rd}$ = 20 d^{-1} is the *MnIV* reduction with sulfide constant,
$K_{\_mn\_rd2}$ = 1 d^{-1} is the *MnIV* reduction with sulfide constant.

4.5.18 Iron (II) oxidation with oxygen:

$$4Fe^{2+} + O_2 + 2H_2O \rightarrow 4Fe^{3+} + 4OH^-$$
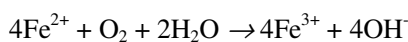
The process of oxidation or iron with oxygen is much faster much faster than that of manganese (Zopfi et al., 2001). Fe reacts with oxygen with a half-life of 1.8 min, and biological catalysis if this reaction is assumed to be unnecessary (Nealson and Stahl, 1997). We assumed:

$fe\_ox=K_{\_fe\_ox}*Fe2*O2$

where $K_{\_fe\_ox}= 4.$ d^{-1} is the Fe oxidation with $O2$ constant.

4.5.19 Iron (II) oxidation by manganese (IV):

$2Fe_2^+ + MnO_2 + 2H_2O \rightarrow FeOOH + Mn^{2+}+ 2H^+$
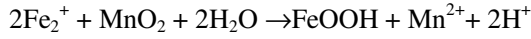
Under anaerobic conditions Fe(II) readily reduces Mn(IV) oxides (Thamdrup et al., 1994). We assumed:

$fe\_mnox=K\_fe\_mnox*Fe2*MnIV$

where $K\_fe\_mnox = 1$ d^{-1} is the Fe oxidation with $MnIV$ constant.

4.5.20 Iron (II) oxidation by nitrate:

For iron oxidation by nitrate (Canfield et al., 2004):

$10Fe^{2+} + 2NO_3^- + 12H^+ = 10Fe^{3+} + N_2 + 6H_2O$
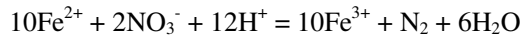
we assumed:

$fe\_nox=K\_fe\_nox*Fe2*NO3$

$K\_fe\_nox = 5$ d^{-1} is the Fe oxidation with $NO3$ constant.

The oxidation of Mn(II) with nitrate was not observed (Neretin et al., 2003).

4.5.21 Iron (III) reduction by sulfide

$2FeOOH + H_2S \rightarrow 2Fe^{2+}+ S^0 + 4OH^-$
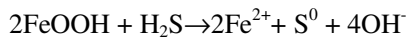
The rates of Fe(III) reduction by *Schewanella Putrefaciens* were found to be 0.02-0.20 h^{-1} (0.48-4.8 d^{-1}) depending on the surface limitation effect for different forms of Fe(III). This process was inhibited by nitrate (Dollhopf et al., 2000). We parameterized it as:

$fe\_rd=K\_fe\_rd*Fe3*H2S$

where $K\_fe\_rd = 0.05$ d^{-1} is the $FeIII$ reduction by sulfide (after Konovalov et al., 2006).

4.5.22 Processes of phosphorus transformation

The transformations of phosphorus species during the synthesis and decay of OM were assumed to follow the Redfield ratios and have been described above. We also included in the model the

processes of co-precipitation and complexation of phosphate connected with the formation and dissolution of oxidized forms of Mn and Fe.

The Fe:P ratio during co-precipitation with iron hydroxides has been reported to be 4 (Savenko, 1995) or 2.7 (T.Leipe, 2006, personal communication). Laboratory experiments show very high ratios of Mn:P = 1000 during co-precipitation of Mn hydroxides (Savenko and Baturin,1996). Therefore phosphorous removal by precipitation of Mn hydroxides was ignored.

It is possible, however, that Mn(III), an intermediate product between Mn(IV) and Mn(II) can play a key role in precipitation of phosphate. Known Mn(III) ligands that bind with enough strength to stabilize Mn(III) in solution include inorganic ligands such as pyrophosphate (Webb et al., 2005), Mn(III)-pyrophosphate complexes are characterized by ratio Mn:P=0.25 for $Mn(HP_2O_7)_2^{3-}$ or Mn:P =0.17 for $Mn(H_2P_2O_7)_3^{3-}$ (Davies, 1969).

In this model we assumed:

Coprecip = (fe_rd - fe_ox- fe_mnox)/2.7 -(mn_ox - mn_ox2 + mn_rd - mn_rd2)/0.66

where coefficient 0.66 is about 4 times greater than the mentioned maximum possible Mn:P ratio, that means that about 25% of Mn(III) should have complexes with polyphosphate. The latter part of Mn(III) can probably form complexes with other ligands.

4.6 Equations for the biogeochemical sources R_C

The main goal of this model was to explain processes in the redox layer processes so we have used a simple model of the living organisms compared with the existing models for the Black (Gregoire et al., 1997; Oguz et al., 1998) and Baltic (Savchuk, 2002; Fennel and Neumann, 2004) Seas. The main role of the *Phy* and *Zoo* modeling compartments was to describe the seasonality of the production of the organic matter. Therefore we did not subdivide these groups. We also assumed that the uptake rate of inorganic nutrients by phytoplankton equals the growth rate of the phytoplankton. Below we describe the formulation for sources R_C for the model compartments as an algebraic sum of reactions that affect the concentrations of the certain compartment. The majority of these reactions for the chemical parameters were descibed above. Here we will present detailed explanation of processes for the biological parameters that were not mentioned earlier.

4.6.1 Biological parameters

Phytoplankton (*Phy*)
The modeled phytoplankton evolved according to:

$$R_{Phy} = GrowthPhy\,(1 - K_{FN}) - MortPhy - ExcrPhy - GrazPhy \quad ,$$

where *GrowthPhy* is the *Phy* specific growth rate; K_{FN}= 0.05 d^{-1} is the specific respiration rate of *Phy*; *MortPhy* is the specific natural mortality rate of *Phy*; *ExcrPhy* is the specific excretion rate of *Phy*; and *GrazPhy* is the loss of *Phy* due to zooplankton grazing.

The phytoplankton specific growth rate,
$$GrowthPhy = K_{NF}\,f_t(t)\,f_i(i)\,min\{\,f_P(PO_4\,),\,f_N(NO_3NO_2\,,NH_4\,)\,\}\ ,$$

is a function of temperature, light and availability of nutrients with with the maximum specific growth rate K_{NF}= 1.86 d^{-1};:

The following formula (Sergeev, 1979) was chosen for dependence on temperature:

$$f_t(t) = 0.2 + 0.22(\exp(0.21t) - 1)/(1 + 0.28\exp(0.21t)) \ .$$

To describe the dependence on light in accordance to (Steel, Frost, 1977):

$$f_i(i) = f_\varphi(\varphi)\frac{I_0}{I_{opt}}\exp(-kh)\exp(1 - \frac{I_0}{I_{opt}}\exp(-kh))$$

we used the following parameters: incident light ($I_0 = 80$), optimal light ($I_{opt} = 25$), extinction coefficient ($k = 0.07$), depth: (h) and variation of light with latitude and time:

$$f_\varphi(\varphi) = \cos(\varphi - 23.5 \sin(2T/365.2)),$$

where T is time (days) and φ is latitude (degrees).

For nutrient limitation parameterization we used a *minimum* function that allowed to switch between limitation on P or N:

$$min \{f(PO_4), f(NO_3,NO_2,NO_3)\}$$

The Michaelis-Menten dependence was used for phosphate limitation description::

$$f(PO_4) = PO_4/(K_{PO4} + PO_4);$$

with K_{PO4}= 0.01 μM, a half-saturation constant for the uptake of PO4 by phytoplankton.
The dependence on nitrogen species was descibed following (Fasham et al., 1990):

$$f_N(NO_3,NO_2,NH_4) = f'_N(NO_3,NO_2) + f''_N(NH_4) = \frac{(NO_3 + NO_2)\exp(-K_{psi}NH_4)}{K_{NO_3} + (NO_3 + NO_2)} + \frac{NH_4}{K_{NH_4} + NH_4}$$

where K_{NH4} =0.02 μM and K_{NO3} =0.20 μM are half-saturation constants for the uptake of NH4 and (NO3+NO2) by phytoplankton. The constant, K_{PSI}=1.46, determines the strength of ammonium inhibition of nitrate uptake.

The excretion rate of *Phy* was described as:

*ExcrPhy=K_{FD}*Phy*

with specific rate of excretion K_{FD} .= 0.05 d^{-1}.

The natural mortality rate of *Phy* was described as:

*MortPhy=K_{FP}*Phy*

with specific rate of mortality $K_{FP.}$=0.05 d^{-1}.

Zooplankton (*Zoo*)

The modeled zooplankton evolved according to:

$R_{Zoo}=Grazing*U_z-MortZoo-K_{ZN}*Zoo$

where *Grazing=GrazPhy+GrazPOP+GrazBact* is the grazing of zooplankton on phytoplankton (*GrazPhy*), detritus (*GrazPOP*) and bacteria (*GrazBact*), U_z= 0.7 is the food absorbency for zooplankton, *MortZoo* is the specific natural mortality rate of *Zoo*; K_{ZN} = 0.1 d^{-1} is the specific respiration rate of *Zoo*.

The grazing of zooplankton on phytoplankton was described with a modified Michaelis-Meten dependence (Ayzatullin, Leonov, 1975):

$GrazPhy=K_{FZ}*Zoo*(Phy/Zoo)/(Phy/Zoo+K_F);$

where
K_{FZ} = 0.5 d^{-1} is the maximum specific rate of grazing of *Zoo* on *Phy,*
K_F = 1 is a half-saturation constant for the grazing of *Zoo* on *Phy* for *Phy*/*Zoo* ratio.

The grazing of zooplankton on phytoplankton was described with a modified Michaelis-Meten dependence (Ayzatulllin, Leonov, 1975):

$GrazPOP=K_{PZ}*Zoo*(POP/Zoo)/(POP/Zoo+K_{PP}/0.001)$

where
K_{PZ} = 0.6 is the maximum specific rate of grazing of *Zoo* on *POP*,
K_{PP} =200 half-saturation constant for the grazing of *Zoo* on *POP* in dependence to ratio *POP*/*Zoo*.

The grazing of *Zoo* on bacteria
$GrazBact= Graz_{B\_ae\_aut} + Graz_{B\_ae\_het} + Graz_{B\_anae\_het} + Graz_{B\_anae\_aut}$
was described as a sum of grazing of the certain groups of bacteria:.

Aerobic autotrophic bacteria:
$Graz_{B\_ae\_aut} =K_{BoaZ}*Zoo*(B\_ae\_aut/Zoo)/(B\_ae\_aut/Zoo+ K_{Boa})$
where
K_{BoaZ}= 0.6 d^{-1} is the maximum specific rate of grazing of *Zoo* on *Baut*,
K_{Boa} = 1.5 is a half-saturation constant for the grazing of *Zoo* on *Baut* for *Baut*/*Zoo* ratio.

Aerobic heterotrophic bacteria:
$Graz_{B\_ae\_het} =K_{BohZ}*Zoo*(B\_ae\_het/Zoo)/(B\_ae\_het/Zoo+ K_{Boh})$
where
K_{BohZ}= 1.02 d^{-1} is the maximum specific rate of grazing of *Zoo* on *Bhet*,
K_{Boh} = 1.1 is a half-saturation constant for the grazing of *Zoo* on *Bhet* for *Bhet*/*Zoo* ratio.

Anaerobic autotrophic bacteria:
$Graz_{B\_anae\_aut} = K_{BaaZ} *Zoo*(B\_an\_aut/Zoo)/(B\_an\_aut/Zoo+ K_{Baa})$
where
K_{BaaZ}= 0.78 d^{-1} is the maximum specific rate of grazing of *Zoo* on *BautA*,

K_{Baa} = 1.5 is a half-saturation constant for the grazing of *Zoo* on *BautA* for *BautA/Zoo* ratio.

Anaerobic heterotrophic bacteria:

$Graz_{B\_anae\_het} = K_{BahZ} * Zoo * (B\_an\_het/Zoo)/(B\_an\_het /Zoo+ K_{Bah})$

where

K_{BahZ}= 0.6 d^{-1} is the maximum specific rate of grazing of *Zoo* on *BhetA*,

K_{Bah} = 1 is a half-saturation constant for the grazing of *Zoo* on *BhetA* for *BhetA/Zoo* ratio.

$MortZoo=K_{ZP}*Zoo*Zoo$ is the zooplankton mortality rate, with maximum specific rate of mortality of zooplankton: K_{ZP}= 0.001 d^{-1} if H$_2$S<20 µM and K_{ZP} = 0.9 d^{-1} if H$_2$S >20 µM.

K_{ZN} =0.10 d^{-1} is the specific rate of respiration of zooplankton.

Aerobic heterotrophic bacteria (*B_ae_het*)

The modeled aerobic heterotrophic bacteria evolved according to:

$R_{B\_ae\_het} = C_{B\_ae\_het} - Mort_{B\_ae\_het} - Graz_{B\_ae\_het}$,

where

$C_{B\_ae\_het} = K_{B\_ae\_het}^{\max} \cdot (DcPM\_O_2 + DcDM\_O_2) \cdot f_{B\_ae\_het}(DON + PON) \cdot B\_ae\_het$ is the growth rate of *B_ae_het,* that we parameterized to be propositionally connected with the rates of aerobic mineralization of particulate ($DcPM\_O_2$) and dissolved ($DcDM\_O_2$) OM.

$K_{B\_ae\_het}^{\max}$ = 2 d^{-1} is the maximum specific growth rate of *B_ae_het*.

$f_{B\_ae\_het}(DON + PON) = \dfrac{PON + DON}{PON + DON+K_{B\_ae\_het}^{N}}$ is the dependence of maximum specific growth rate of *B_ae_het* on POM and DOM content,

$K_{B\_ae\_het}^{N}$ = 0.5 µM is a half-saturation constant for the dependence of maximum specific growth rate of *B_ae_het* on POM and DOM content.

$Mort_{B\_ae\_het} = K_{B\_ae\_het}^{Mort}B\_ae\_het^2$ is the rate of mortality of *B_ae_het*, with maximum specific rate of mortality:

$K_{B\_ae\_het}^{Mort}$ = 0.03 d^{-1} if O_2>1 µM and $K_{B\_ox\_het}^{Mort}$ =0.99 d^{-1} if O_2< 1 µM.

$Graz_{B\_ae\_het}$ is the grazing of *Zoo* on *B_ae_het*.

Aerobic autotrophic bacteria (*B_ae_aut*)

The modeled aerobic autotrophic bacteria evolved according to:

$R_{B\_ae\_aut} = C_{B\_ae\_aut} - Mort_{B\_ae\_aut} - Graz_{B\_ae\_aut}$,

where

$$C_{B\_ae\_aut} = K_{B\_ae\_aut}^{\max} \cdot (Nitrif1 + Nitrif2 + S^0\_ox + S_2O_3\_ox + mn\_ox + fe\_ox)$$
$$\cdot f_{B\_ae\_aut}^{NP}(NH_4, PO_4) \cdot B\_ae\_aut$$

is the growth rate of *B_ae_aut,* connected with nitrification and oxidation by O_2 of reduced species of *S, Mn* and *Fe*. These processes are usually considered as autotrophic (Canfield et al., 2005).

$K_{B\_ae\_aut}^{\max}$ = 1 d^{-1} is the maximum specific growth rate of *B_ae_aut*.

$$f_{B\_ae\_aut}^{NP}(NH_4, PO_4) = \min\left\{ \frac{NH_4}{NH_4 + K_{B\_ae\_aut}^{N}} \frac{PO_4}{PO_4 + K_{B\_ae\_aut}^{P}} \right\}$$ is the dependence of maximum

specific growth rate of *B_ae_het* on *NH_4* and *PO_4,*

where:

$K_{B\_ae\_aut}^{N}$ = 0.05 μM and $K_{B\_ae\_aut}^{P}$ = 0.3 μM are half-saturation constants for the dependence of maximum specific growth rate of *B_ae_aut* on NH4 and PO4 content.

$Mort_{B\_ae\_aut} = K_{B\_ae\_aut}^{Mort} B\_ae\_aut^2$ - is the rate of mortality of *B_ae_aut* with maximum specific rate of mortality:

$K_{B\_ae\_aut}^{Mort}$ = 0.1 d^{-1} if O_2>1 μM and $K_{B\_ae\_aut}^{Mort}$ = 0.99 d^{-1} if O_2< 1 μM.

$Graz_{B\_ae\_aut}$ is the grazing of *Zoo* on *B_ae_aut.*

Anaerobic heterotrophic bacteria (*B_anae _het*)

The modeled anaerobic heterotrophic bacteria evolved according to:

$$R_{B\_anae\_het} = C_{B\_anae\_het} - Mort_{B\_anae\_het} - Graz_{B\_anae\_het},$$

where

$$C_{B\_anae\_het} = K_{B\_anae\_het}^{\max}(DcPM\_NO_3 + DcDM\_NO_3 + DcPM\_SO_4 +$$
$$+ DcDM\_SO_4) f_{B\_anae\_het}(DON + PON) B\_anae\_het$$

is the growth rate of *B_anae_het* connected with denitrification and sulfate reduction of POM and DOM. The rate of growth of sulfate reduction bacteria can be very fast (with doubling times 4h) (Canfield et al., 2005)..

$K_{B\_anae\_het}^{\max}$ = 2 d^{-1} is the maximum specific growth rate of *B_anae_het* .

$$f_{B\_anae\_het}(DON + PON) = \frac{PON + DON}{PON + DON + K_{B\_anae\_het}^{N}}$$ - is the dependence of maximum specific

growth rate of *B_anae_het* on OM content,

28

$K^N_{B\_anae\_het}$ = 6 μM is a half-saturation constant for the dependence of maximum specific growth rate of *B_anae_het* on POM and DOM content.

$Mort_{B\_anae\_het} = K^{Mort}_{B\_anae\_het}B\_anae\_het^2$ is the rate of mortality of *B_ae_het* with maximum specific rate of mortality:

$K^{Mort}_{B\_anae\_het}$ =0.01 d^{-1}.

$Graz_{B\_anae\_het}$ is the grazing of *Zoo* on *B_anae_het*.

Anaerobic autotrophic bacteria (*B_anae_aut*)

The modeled anaerobic heterotrophic bacteria evolved according to:

$R_{B\_anae\_aut} = C_{B\_anae\_aut} - Mort_{B\_anae\_aut} - Graz_{B\_anae\_aut}$,

where:

$$C_{B\_anae\_aut} = K^{\max}_{B\_anae\_aut}(mn\_rd + fe\_rd + hs\_ox + hs\_no3 + hs\_no2 + \\ + anammox)f^{NP}_{B\_anae\_aut}(NH_4, PO_4)B\_anae\_aut$$

is the growth rate of *B_anae_aut* connected with Mn reduction, Fe reduction, H$_2$S oxidation by O$_2$, NO$_3$ and NO$_2$, and anammox. These processes are usually considered as autotrophic, as is disproportionation of S^0 (Jost et al., in press).

$K^{\max}_{B\_anae\_aut}$ =6.5 d^{-1} is the maximum specific growth rate of *B_anae_aut*.

$$f^{NP}_{B\_anae\_aut}(NH_4, PO_4) = \min\left\{\frac{NH_4}{NH_4 + K^N_{B\_anae\_aut}}\frac{PO_4}{PO_4 + K^P_{B\_anae\_aut}}\right\}$$ is the dependence of

maximum specific growth rate of *B_anae_aut* on *NH$_4$* and *PO$_4$,*, where:

$K^N_{B\_anae\_aut}$ = 3 μM and $K^P_{B\_anae\_aut}$ = 3 μM are half-saturation constants for the dependence of maximum specific growth rate of *B_ae_aut* on ammonia and phosphate content.

$Mort_{B\_anox\_aut} = K^{Mort}_{B\_anox\_aut}B\_anox\_aut^2$ is the rate of mortality of *B_anox_aut* with maximum specific rate of mortality

$K^{Mort}_{B\_anae\_aut}$ =0.001 d^{-1} if H$_2$S <16 μM and $K^{Mort}_{B\_anae\_aut}$ = 0.99 d^{-1} if H$_2$S > 16 μM.

$Graz_{B\_anae\_aut}$ is the grazing of *Zoo* on *B_anae_het*.

The mortality of aerobic autotrophic bacteria was assumed to be dependent on H$_2$S because from observations in the Baltic Sea (M.Labrenz, 2005 p.c.) and in the Black Sea (82th cruise of RV "Akvanavt") an abrupt decrease of dark CO$_2$ fixation is marked at about H$_2$S > 20 μM.

4.6.2 Chemical parameters

Below we list the formulation for sources R_C for the chemical compartments of the model as an algebraic sum of reactions described above.

Phosphate (*PO4*)

$R_{PO4}=Sp(GrowthPhy(K_{FN}-1.)-Chemos-ChemosA+K_{ZN}Zoo) +PhosPOP+PhosDOP +Coprecip$

Dissolved Organic Phosphorus (*DOP*)

$R_{DOP}=Sp(ExcrPhy+Grazing(1.-U_z)H_z+0.7MortBact-(Hetero+HeteroA)$
$-DON/(DON+PON)(Hetero+HeteroA))+AutolisP-PhosDOP$
where H_z=0.6 is the ratio between dissolved and particulate excretes of zooplankton.

Particulate Organic Phosphorus (*POP*)

$R_{POP}=Sp(MortPhy+MortZoo+0.3MortBact+Grazing(1.-U_z)(1.-Hz)-GrazPOP-$
$PON/(DON+PON)*(Hetero+HeteroA))-AutolisP-PhosPOP$

Particulate Organic Nitrogen (*PON*)

$R_{PON}=Sn(MortPhy+MortZoo+0.3MortBact+Grazing(1.-U_z)(1.-H_z)-GrazPOP$
$-PON/(DON+PON)(Hetero+HeteroA))-AutolisN-AmmonPON$

Dissolved Organic Phosphorus (*DON*)

$R_{DON}=Sn(ExcrPhy+Grazing(1.-U_z)H_z+0.7MortBact$
$-(Hetero+HeteroA)) +AutolisN-AmmonDON$

Ammonia (*NH4*)

$R_{NH4}=Sn*(GrowthPhy(K_{FN}-1.)(LimNH4/LimN)-Chemos-ChemosA+K_{ZN}*Zoo)$
$+AmmonPON+AmmonDON-Nitrif1+Nfixation$

Nitrite (*NO2*)

$R_{NO2}=Sn*(GrowthPhy*(K_{FN}-1.)*(LimNO3/LimN)*(NO2/(NO2+NO3)))+Nitrif1-Nitrif2$
$+Denitr1–Denitr2–sulfido2$

Nitrate (*NO3*)

$$R_{NO3} = Sn*(GrowthPhy*(K_{FN}-1.)*(LimNO3/LimN)*(NO3/(NO2+NO3)))+Nitrif2-Denitr1$$
$$-1.25sulfido - mn\_nox\text{-}fe\_nox$$

Oxygen (*O2*)

$$R_{O2} = OkP\ Sp\ GrowthPhy\ +2.Sn\ GrowthPhy(NO3/(NO2+NO3))(LimNO3/LimN)$$
$$+0.5Sn\ GrowthPhy\ (NO2/(NO2+NO3))(LimNO3/LimN)\ -\!-\ Destr\_OM$$
$$-\ OkP\ Sp(GrowthPhy\ KFN+KZN\ Zoo)-1.5Nitrif1-0.5Nitrif2-0.5hs\_ox$$
$$-\ 1.s0\_ox - 2.s23\_ox - 1.mn\_ox - fe\_ox$$

Hydrogen sulfide (*H2S*)

$$R_{H2S} = -hs\_ox + s23\_rd - 0.5fe\_rd - mn\_rd - sulfido - sulfido2 +0.5Disprop$$

Elemental sulfur (*S0*)

$$R_{S0} = hs\_ox - s0\_ox + 1.mn\_rd - Disprop$$

Thiosulfate (*H2S*)

$$R_{S2O3} = s0\_ox - s23\_ox + s4\_rd - s23\_rd +0.5Disprop$$

Sulfate (*SO4*)

$$R_{SO4} = s23\_ox - s4\_rd + sulfido+sulfido2$$

Bivalent manganese (*MnII*)

$$R_{MnII} = mn\_rd2 - mn\_ox +0.5*fe\_mnox$$

Trivalent manganese (*MnIII*)

$$R_{MnIII} = mn\_ox - mn\_ox2 + mn\_rd - mn\_rd2$$

Quadrivalent manganese (*MnIV*)

$$R_{MnIV} = mn\_ox2 - mn\_rd -0.5*fe\_mnox$$

Bivalent iron (*FeII*)

R_{FeII} = fe_rd - fe_ox - fe_mnox -5.*fe_nox

Trivalent iron (*FeIII*)

R_{FeIII} = fe_ox + fe_mnox + 5.*fe_nox- fe_rd

The complete list of the model coefficients is presented in Table 2.

Table 2. Parameters names, notations, values and units of the coefficients used in the model.

Parameter	Notation	Value
Specific rate of decomposition of *POM* to *DOM*	K_{PD}	0.10 d^{-1}
Mineralization in oxic conditions		
Specific rate of decomposition of *DON*	K_{ND4}	0.1 d^{-1}
Specific rate of decomposition of *PON*	K_{NP4}	0.04 d^{-1}
Temperature parameter for oxic mineralization	*Ktox*	0.15 ^{o}C^{-1}
Oxygen parameter for oxic mineralization	*O2ox*	0 μM
Oxygen parameter for oxic mineralization	*Kox*	15 μM
Denitrification		
Specific rate of 1st stage of denitrification	K_{N32}	0.12 d^{-1}
Specific rate of 2d stage of denitrification	K_{N24}	0.20 d^{-1}
Oxygen parameter for denitrification	*O2dn*	25 μM
NO3 parameter for denitrification	*NO3mi*	1*10^{-3} μM
NO2 parameter for denitrification	*NO2mi*	1*10^{-4} μM
Sulfate reduction		
Specific rate of sulfate reduction with sulfate	K_{s4_rd}	2.5*10^{-7} d^{-1}
Specific rate of sulfate reduction with thiosulfate	K_{s23_rd}	1.2 d^{-1}
Oxygen parameter for sulfate reduction	*O2sr*	25 μM
NO3 and *NO2* parameter for sulfate reduction	*NOsr*	0.5 μM
Nitrification		
Specific rate of the 1st stage of nitrification	K_{N42}	0.9 d^{-1}
Specific rate of the 2d stage of nitrification	K_{N23}	2.5 d^{-1}
Oxygen parameter for nitrification	*O2nf*	1 μM
Nitrogen fixation		
Specific rate of nitrogen fixation	K_{Nfix}^{max}	20 d^{-1}
Anammox		
Anammox constant	$K_{annamox}$	0.03 d^{-1}
Oxidation of the hydrogen sulfide		
Specific rate of oxidation of *H2S* with *O2*	K_{hs_ox}	0.2 d^{-1}
Specific rate of oxidation of *S0* with *O2*	K_{s0_ox}	4.0 d^{-1}
Specific rate of oxidation of *S2O3* with *O2*	K_{s23_ox}	1.5 d^{-1}
S0 disproportionation		
Specific rate of *S0* disproportionation	*Kdisp*	0.01 d^{-1}
Thiodenitrification		

Thiodenitrification constant	K_T	0.8 μM^{-1}d^{-1}
Oxidation and reduction of Mn and Fe		
MnII oxidation with *O2* constant	$K_{\_mn\_ox}$	2 d^{-1}
MnIV reduction with Sulfide constant	$K_{\_mn\_rd}$	22 d^{-1}
MnIII oxidation with *O2* constant	$K_{\_mn\_ox2}$	18 d^{-1}
MnIV reduction with Sulfide constant	$K_{\_mn\_rd2}$	2 d^{-1}
Fe oxidation with *O2* constant	$K_{\_fe\_ox}$	4. d^{-1}
Fe oxidation with *MnIV* constant	$K_{\_fe\_mnox}$	1 d^{-1}
Fe oxidation with *NO3* constant	$K_{\_fe\_nox}$	5. d^{-1}
FeIII reduction by sulfide	$K_{\_fe\_rd}$	0.05 d^{-1}
Phytoplankton		
Maximum specific growth rate	K_{NF}	1.86 d^{-1}
Specific respiration rate	K_{FN}	0.05 d^{-1}
Incident light	I_0	80
Optimal light	I_{opt}	25
Extinction coefficient	K	0.07
Half-saturation constant for uptake of *PO4*	K_{PO4}	0.01 μM
Strength of ammonium inhibition of nitrate uptake constant	K_{psi}	1.46
Half saturation constant for uptake of *NH4*	K_{NH4}	0.02 μM
Half saturation constant for uptake of *NO3+NO2*	K_{NO3}	0.03 μM
Specific rate of mortality	K_{FP}	0.05 d^{-1}
Specific rate of excretion	K_{FD}	0.05 d^{-1}
Zooplankton		
Specific respiration rate	K_{ZN}	0.1 d^{-1}
Maximum specific rate of grazing of *Zoo* on *Phy*	K_{FZ}	0.5 d^{-1}
Half-saturation constant for the grazing of *Zoo* on *Phy* for *Phy*/*Zoo* ratio	K_F	1
Maximum specific rate of grazing of *Zoo* on *POP*	K_{PZ}	0.6 d^{-1}
Half-saturation constant for the grazing of *Zoo* on *POP* in dependence to ratio *POP*/*Zoo*	K_{PP}	200
Maximum specific rate of grazing of *Zoo* on *Baut*	K_{BoaZ}	0.6 d^{-1}
Half-saturation constant for the grazing of *Zoo* on *Baut* for *Baut*/*Zoo* ratio	K_{Boa}	1.5
Maximum specific rate of grazing of *Zoo* on *Bhet*	K_{BohZ}	1.02 d^{-1}
Half-saturation constant for the grazing of *Zoo* on *Bhet* for *Bhet*/*Zoo* ratio	K_{Boh}	1.1
Maximum specific rate of grazing of *Zoo* on *BautA*	K_{BaaZ}	0.78 d^{-1}
Half-saturation constant for the grazing of *Zoo* on *BautA* for *BautA*/*Zoo* ratio	K_{Baa}	1.5
Maximum specific rate of grazing of *Zoo* on *BhetA*	K_{BahZ}	0.6 d^{-1}
Half-saturation constant for the grazing of *Zoo* on *BhetA* for *BhetA*/*Zoo* ratio	K_{Bah}	1
Maximum specific rate of mortality of *Zoo*	K_{ZP}	0.001 d^{-1} if:H_2S<20 μM 0.9 d^{-1} if:H_2S>20 μM

Food absorbency for zooplankton	Uz	0.7
Ratio between dissolved and particulate excretes of zooplankton	H_z	0.6
Aerobic heterotrophic bacteria		
Maximum specific growth rate of *B_ae_het*	$K_{B\_ae\_het}^{\max}$	2 μM^{-1}
Half-saturation constant for the dependence of maximum specific growth rate of *B_ae_het* on POM and DOM content.	$K_{B\_ae\_het}^{N}$	0.5 μM
Maximum specific rate of mortality of *B_ae_het*	$K_{B\_ae\_het}^{Mort}$	0.03 d^{-1} If: $O_2>1\mu M$ 0.99 d^{-1} If: $O_2<1\mu M$
Aerobic autotrophic bacteria		
Maximum specific growth rate of *B_ae_aut*	$K_{B\_ae\_aut}^{\max}$	1 μM^{-1}
Half-saturation constant for the dependence of maximum specific growth rate of *B_ae_aut* on NH4	$K_{B\_ae\_aut}^{N}$	0.05 μM
Half-saturation constants for the dependence of maximum specific growth rate of *B_ae_aut* on PO4	$K_{B\_ae\_aut}^{P}$	0.3 μM
Maximum specific rate of mortality of *B_ae_aut*	$K_{B\_ae\_aut}^{Mort}$	0.01 d^{-1} If: $O_2>1\mu M$ 0.99 d^{-1} If: $O_2<1\mu M$
Anaerobic heterotrophic bacteria		
Maximum specific growth rate of *B_anae_het*	$K_{B\_anae\_het}^{\max}$	2 μM^{-1}
Half-saturation constant for the dependence of maximum specific growth rate of *B_anae_het* on POM and DOM	$K_{B\_anae\_het}^{N}$	6 μM
Maximum specific rate of mortality of *B_anae_het*	$K_{B\_anae\_het}^{Mort}$	0.01 d^{-1}
Anaerobic autotrophic bacteria		
Maximum specific growth rate of *B_anae_aut*	$K_{B\_anae\_aut}^{\max}$	6.5 μM^{-1}
Half-saturation constants for the dependence of maximum specific growth rate of *B_ae_aut* on NH4	$K_{B\_anae\_aut}^{N}$	3 μM
Half-saturation constants for the dependence of maximum specific growth rate of *B_ae_aut* on PO4	$K_{B\_anae\_aut}^{P}$	3 μM
Maximum specific rate of mortality of *B_anae_aut*	$K_{B\_anae\_aut}^{Mort}$	0.001 d^{-1} if $H_2S <16\ \mu M$ 0.99 d^{-1} if $H_2S <16\ \mu M$

5. Computational aspects

A code of this model was written in Visual Fortran 90 for PC Windows. The calculations were started from the uniform distribution of the considered variables. We conducted numerical integration with Euler scheme with process splitting. The time steps were 0.00125 d^{-1} for diffusion and 0.0025 d^{-1} for biogeochemical processes and sedimentation. The vertical resolution was 2 m. A quasi-stationary solution with the seasonal forced oscillations was reached. There were no changes of the year-averaged concentrations of the variables for at least 100 model years.

6. Results of simulations

We made the basic model simulations of the redox layer development under the seasonal changes forcing for the Black Sea hydrophysical scenario described above. The calculated vertical distributions of the model variables for the summer period are presented in Fig. 5.
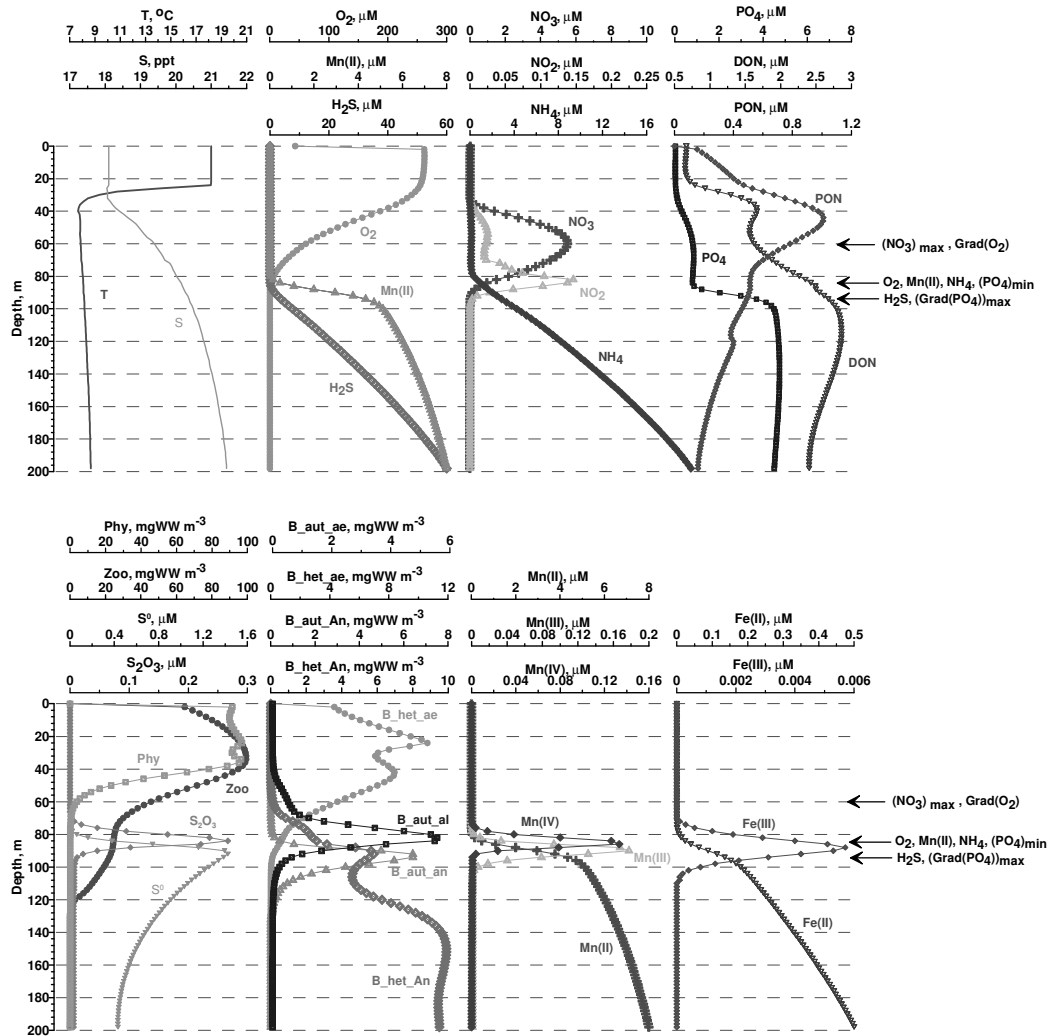
Fig. 5. Results of the model calculation of the vertical distribution of the parameters in summer

In Table 3 we give the rates of the key processes, responsible for the structure of the redox layers calculated in this model and estimated on the basis of observations and experiments in the Black and Baltic Seas.

For verification of the model it is possible to compare the results of simulations with (i) the observed distributions of the concentrations of variables and the (ii) results of measurements of the rates of processes.

Here we will discuss these features.

6.1 Variables

In the model, the dissolved oxygen structure is characterized by a uniform distribution in the upper mixed layer (270 μM), the presence of a pronounced oxycline with the vertical gradient of 7 μM m^{-1} (between 40 and 70 m) and decrease of the vertical gradient in the deeper layers (Fig. 5). Oxygen reaches zero concentrations (less than 0.5 μM) at a depth about 85 m.

The vertical profiles of nitrogen compounds (NH_4, NO_2, NO_3) calculated by the model reflect the main features of the distributions of these compounds observed in nature. Nitrate concentrations in the maximum layer reach 4.5 μM both in model and in nature. The NO_2 maximum peak is situated at approximately the same depth where the concentrations of NH_4 and NO_3 are equal.

H_2S appears about 5-10 m below the onset of the increase in NH_4, S^0 is characterized by maximum absolute values (1.5 μM) at the depth of appearance of H_2S (concentrations in the Black Sea 0.1 - 5.4 μM: Volkov, 1992). Concentrations of S_2O_3, an intermediate product of both sulfate reduction and sulphide oxidation, are uniform with a small maximum of 0.2 μM at a depth slightly above the H_2S onset. The model calculated maximum of S^0 was smaller than was observed in the Baltic Sea – 4 μM. The vertical gradient of H_2S in the model changes from 0.66 to 0.5 μM m^{-1} with the maximum gradient several meters below the onset (compare to 0.63 μM m^{-1} according to Volkov et al., 1992).

Profiles of manganese compounds derived from the model also reflect the basic features of this parameter's vertical distribution in nature. Mn(II) onset occurs at the same depth as the NH_4 onset. The modeled vertical gradient of dissolved Mn(II) increase shallower the H_2S onset is about 0.6 μM m^{-1}, while smaller values (0.3 – 0.5 μM m^{-1}) were seen in the field data (Pakhomova, 2005; Yakushev et al., 2002). In the model Mn(IV) concentrations reached 0.1-0.2 μM in the zone between the onset of oxygen and hydrogen sulfide. These values are in agreement with the data received for both the Black (Erdogan et al., 2003) and the Baltic (Neretin et al., 2003) Seas. The model calculated Mn(III) concentrations correspond to the measured by Trouwborst et al. (2006).

The vertical distribution of Fe was similar to that of Mn. The maximum concentrations of Fe(III) (0.01 μM) in the model corresponded to the observations (Pakhomova, 2005) and were found deeper that the Mn(IV) maximum. Therefore the modeled "iron interface" is slightly deeper than "manganese interface" as is observed in nature (Lewis and Landing, 1991).

The PO_4 distribution in the model reflected the main features of the observed data (Fig. 1, 3). The problems of the formation of the phosphate distribution will be discussed below.

The model calculated concentrations of PON and DON (correspondingly 0.3-2.0 μM and 2-5 μM) are lower than observed in the Black Sea (Konovalov et al., 2006; Yakushev et al., 2006) and the Baltic Sea (2.9 μM and 14.6 μM, Nagel, p.c., 2006). That can be explained by the fact that this model computes only autochthonous OM and doesn't consider the allocthonous material that derives from rivers (and during North Sea water influx events in the Baltic Sea).

The biological characteristics (biomasses of phytoplankton and zooplankton) varied from 50 to 250 mg m^{-3} depending on the season in the model in an agreement with the observations for the Black Sea (Sorokin, 2002). The calculated biomass of bacteria in the redox-zone (5-10 mg m^{-3}) on the whole corresponded to the observed values as well (Pimenov and Neretin, 2006).

In general the model calculated vertical structure reflects the basic features of structure of the redox layers of the studied seas. In particular (i) the correspondence of depth of the nitrate maximum with changing of O_2 concentrations, (ii) the similarity of the depth of onsets of Mn(II) and NH_4 and (iii) the position of the H_2S onset and a layer with maximum gradients of phosphate several meters below. Therefore the model confirms that the sequences in vertical profile of disappearance of electron acceptors ($O_2 \rightarrow NO_3 \rightarrow Mn(IV) \rightarrow Fe(III)$) and appearance of electron donors (Mn(II) $\rightarrow NH_4 \rightarrow Fe(II) \rightarrow H_2S$) corresponds to the sequences of the couples' electron potentials in the theoretical "electron tower" (Canfield et al., 2005). The model maxima of Mn(IV), Fe(III) and anaerobic autotrophic bacteria correspond to the turbidity layer depth.

6.2 Processes.

Absolute values of primary production and dark CO_2 fixation (Table 1) correspond to the observations data. The calculations confirm that the primary maximum of chemosynthesis has to be formed below the hydrogen sulfide boundary (Fig. 5). The less pronounced secondary maximum is observed about 5-10 m shallower than the hydrogen sulfide boundary and is likely to be connected with nitrification. These results are in agreement with observations in the Black Sea (Pimenov and Neretin, 2006) and the Baltic Sea. The model calculated maximum rate of chemosynthesis (0.5-1.0 μM C l^{-1}) corresponded well to the results of measurements (Table 2). According to Jost et al. (in press) chemosynthesis with values 0.8-1.0 μM C l^{-1} is found in the Baltic Sea in a 0-20 m layer beneath the sulfide boundary.

Table 4. Comparison of the rates of biogeochemical processes in model, Black Sea and Baltic Sea.

Process (units)	Model	Black Sea	Baltic Sea
Primary Production ($g\ C\ m^{-2}\ yr^{-1}$)	$90\ g\ C\ m^{-2}\ yr^{-1}$	$40\text{-}90\ g\ C\ m^{-2}\ yr^{-1}$ (Finenko, 1979, Sorokin, 1993), $150\ g\ C\ m^{-2}\ yr^{-1}$ (Vedernikov, Demidov, 1993)	$150\ g\ C\ m^{-2}\ yr^{-1}$ (Wasmund et al., 2001)
Dark CO_2 fixation ($\mu M\ C\ d^{-1}$)	0.3-0.7	0.2 (Pimenov, Neretin 2006), 0.25 (Sorokin, 2002), 0.4-2 (Yilmaz et al., 2006), $2.3\text{-}7.7\ \mu g\ C\ L^{-1}d^{-1}$ (Morgan et al., 2006)	0.8-1.0 (Jost, p.c. 2006)
Sulfide oxidation ($\mu M\ S\ d^{-1}$)	1.9	0.3 -4.5 (Sorokin, 1992, Bezborodov, Eremeev, 1993, Jorgensen et al., 1991, Sorokin, 2002)	
S^0 oxidation ($\mu M\ S\ d^{-1}$)	0.3	for S^0 oxidation 0.6-0.9 (Sorokin et al., 1992), 10-33 mg S $l^{-1}\ d^{-1}$ (Sorokin, 2002), for S_2O_3 oxidation 0.2-0.6 (Sorokin et al., 1992, 2002)	
Sulfate reduction ($\mu M\ S\ d^{-1}$)	0.02	0.003-0.03 (Gulin, 1989); 0.03-0.13 (Lein et al., 1990); 0.04-1.7 (Il'chenko and Sorokin, 1991); 0.003-0.036 (Jorgensen et al., 1991); 0.02-0.3 (Sorokin et al., 1992); 0.000008-0.0035 (Albert et al., 1995). 0.0035 (Canfield et al., 2005), 0.2-0.6 (Pimenov, Neretin, 2006)	
Ammonification in oxic zone ($\mu M\ N\ d^{-1}$)	0.1-0.5	0.1-0.5 (calculated on the data of Sorokin et al., 1991), 0.005-0.05 (Kuypers et al., 2003)	
Nitrification, ($\mu M\ N\ d^{-1}$)	0.2 0.75 (deep NO_2 max)	NH4 oxidation – 0.005-0.05 (Ward, Kilpatrick, 1991), 0.02-0.05 (Sorokin, 2002) NO2 oxidation - 0.05-0.24 (Ward, Kilpatrick, 1991) 0.002-0.2 in the coastal regions of the Ocean (Canfield et al., 2005)	0.001-0.28 (Enoksson, 1986) 0.017-0.48 (Bauer, 2003)
Denitrification ($\mu M\ N\ d^{-1}$)	0.2	0.002 (Ward and Kilpatrick, 1991). 0.7-4 in the coastal regions of the Ocean (Canfield et al., 2005)	$0\ \mu M\ N_2\ d^{-1}$ (Hannig et al, 2006) 0.044-0.11 (Brettar & Rheinheimer 1991)
Nitrogen fixation ($\mu M\ N\ d^{-1}$)	0.1-0.5	0.02-0.04 ($0.60\text{-}1.16\ mg\ N\ m^{-3}d^{-1}$) (Sorokin, 2002)	$0.08\text{-}2.3\ mmol\ N\ m^{-2}\ d^{-1}$ (Wasmund et al. 2005) $0.68\text{-}0.74\ mmol\ N\ m^{-2}\ d^{-1}$ (Stal, Walsby 2000)
Thiodenitrification ($\mu M\ N\ d^{-1}$)	0.2	is possible (Sorokin, 2002)	$0\text{-}2.7\ \mu M\ N_2\ d^{-1}$ (Hannig et al, 2006)
Anammox ($\mu M\ N\ d^{-1}$)	0-0.03	0.007 (Kuypers et al., 2003)	0-0.05 (Hannig et al, 2006)
Mn oxidation $\mu M\ Mn\ d^{-1}$	1.0	0.02-0.8 (Neretin, p.c.) 0.18-1.9 (Tebo, 1991)	
Mn reduction	0.9	0.96-3.6 (Nealson et al., 1991)	

The ratio between the annually integrated rate of photosynthesis to the rate of chemosynthesis in the model was about 15%, corresponding to estimates that the chemoautotrophic production rates were 10-32% of surface photoautotrophic production in the Black Sea (Yilmaz et al., 2006). The similar ratio is known for the Baltic Sea.

The processes of the sulfide oxidation and sulfate reduction in the model corresponded well to the results of observations known for the Black Sea (Table 4).

The rate of ammonification obtained in the model is similar to the values obtained by Sorokin (2002), but is much higher than the estimates by Kuypers et al. (2003). Nitrification calculated in the model was close to the values known for the Baltic and Black Seas (Table 4). Modeled denitrification was larger than observed, while thiodenitrification was at the limit of possible values for the Baltic Sea. Modeled values of anammox corresponded well to the observations results. The rate of the nitrogen fixation in the model was twice as large as measured in the Black Sea.

The processes of manganese oxidation (1.0 μM Mn d^{-1}) and manganese reduction (0.9 μM Mn d^{-1}) corresponded well to the results of observations (Table 4).

Generally the model's estimates fit well to the observed values of the processes, but some differences occur. These differences probably can be explained by the fact that the model represents the averaged balanced picture, while, during observations, the rates of processes could depend on a transient situation, connected with subsequences of intrusions or temporal variability. In addition, the vertical resolution of sampling and the weather conditions during the field studies can play a significant role in the agreement of the sampled data to the complete situation in nature. Redox zone processes can occur within thin 2-3 m layers (Murray et al., 1995, Yakushev et al., 2002), and it is practically impossible to sample, for example from a 2-m wide nitrite maximum in rough weather conditions because of the ship movements. An intensive study of anammox in the last 5 years revealed that this processes is not found at all times or in all locations (Hannig et al., 2006, Kilpatrick, 2005, p.c.).

7. Discussion

One of the main goals of the using of models is to apply them for the analysis of the observations. It was shown in the previous section, that the calculated spatial and temporal distributions of parameters agree reasonably well with the results of observations. The degree of this agreement allows us to believe to the results of other analyses that can be completed with the model. We will present here the examples of application of ROLM for some specific questions about the redox layer functioning.

7.1 Oxidation of H$_2$S.

Oxidation of the hydrogen sulfide is probably the primary current problem of biogeochemistry of the marine redox interfaces, because from the 1990^s, it became evident that the potential sink of H$_2$S is not balanced solely by O$_2$ supply. It is generally assumed that the oxidation of H$_2$S is connected with the activity of chemolithotrophic bacteria (Zopfi et al, 2001). However, the chemical oxidation of sulfides plays a dominant role when both of H$_2$S and O$_2$ are present in large concentrations (Zopfi et al, 2001).

On one hand, experiments with labeled S demonstrate that this process has a maximum rate at about 0-20 m below the sulfide onset, but on the other hand, the electron acceptor of this reaction has not been identified experimentally
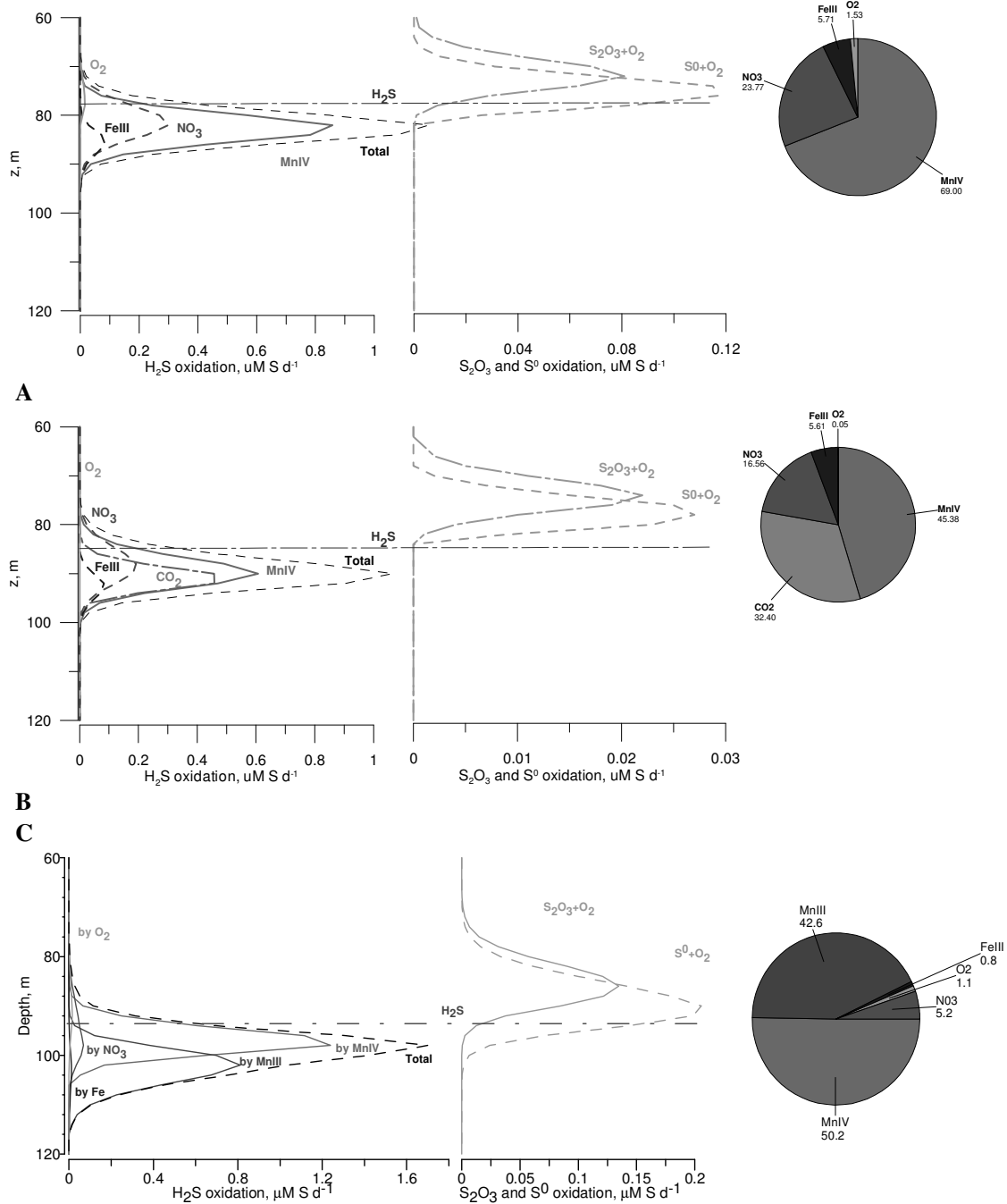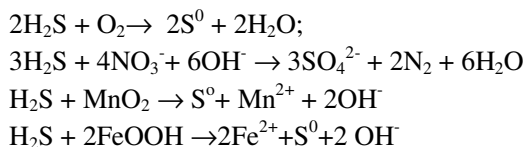

Fig. 6. The left column represents the rates of oxidation of hydrogen sulfide with *O2, NO3, MnIV, FeIII* (A), *O2, NO3, MnIV, FeIII, CO2* (B) and *O2, NO3, MnIV, MnIII, FeIII* (C). Middle column represent corresponding rates of oxidation of *S0* and *S2O3* with *O2* and the right column shows the shares of considered electron-acceptors in the process of sulfide oxidation.

below the sulfide interface (Murray et al., 1995; Yakushev et al., 2002; Stunzhas 2000). The maximum dark CO_2 fixation is also observed in the 10-20 m layer below the sulfide interface (Pimenov and Neretin, 2006)).

We used the model to analyze the possible role of different electron-acceptors. The oxidation of H_2S in the model occurred through the following reactions:

$2H_2S + O_2 \rightarrow 2S^0 + 2H_2O$;
$3H_2S + 4NO_3^- + 6OH^- \rightarrow 3SO_4^{2-} + 2N_2 + 6H_2O$
$H_2S + MnO_2 \rightarrow S^o + Mn^{2+} + 2OH^-$
$H_2S + 2FeOOH \rightarrow 2Fe^{2+} + S^0 + 2OH^-$

The modeled vertical profiles of these processes rates are presented in Fig. 6A.

According to the model estimates the oxidation of H_2S with O_2 was very slow (less than 0.01 µM d^{-1} (or 0.02 µM S d^{-1}). The maximum rates of Mn reduction were 0.8 µM d^{-1}, Fe reduction 0.10 µM d^{-1} and NO_3 reduction about 0.30 µM d^{-1} . Therefore the oxidation of H_2S was due primarily to reduction of Mn(IV) - 69.0%, NO_3 - 23.8%, Fe(III) - 5.7 %, and O_2 -1.5% (Fig. 6A).

The oxidation of the elemental sulfur and thiosulfate to sulfate occurs with dissolved oxygen several meters shallower (Fig. 6, central column).

Besides the mentioned reactions, anoxygenic photosynthesis (Overmann and Manske, 2006) can also result in the oxidation of H_2S (Canfield et al., 2005):

$2H_2S + CO_2 \rightarrow CH_2O + 2S^0 + H_2O$ or
$H_2S + 2CO_2 + 2H_2O \rightarrow 2CH_2O + SO_4^{2-} + 2H^+$
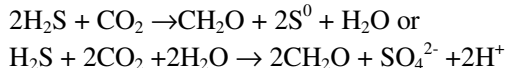
With this model we made simulations that parameterize all the dark CO_2 fixation as connected with these processes. Results are presented in Fig. 6B. In this case the consumption of CO_2 should result, in oxidation of 0.1- 0.5 µM S d^{-1}. This is a significant share of the total sulfide oxidation (32.4 %) but the share of sulfide oxidized with Mn(IV) remained highest.

In the last version of this model we considered the Mn reduction through an intermediate Mn(III):

$2Mn^{4+} + HS^- + OH^- \rightarrow 2Mn^{3+} + S^0 + H_2O$
$2Mn^{3+} + HS^- \rightarrow 2Mn^{2+} + S^0 + H^+$
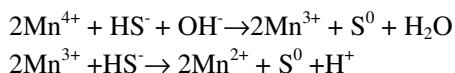
In this case the sulfide oxidation is due to reduction of Mn(IV) – 50.2%, Mn(III) – 42.6%, NO_3 – 5.2%, Fe(III) – 0.8 %, and O_2 - 1.1% (Fig. 6C).

All these numerical experiments can reflect specific situations in natural waters, connected with either stable situations, or following intrusions. The role of anoxygenic photosynthesis should change due to or shallower or deeper position of the redox-interface. But in any case the dominant role in oxidation of sulfide seems to belong to the oxidized Mn species.

This model suggest that particulate Mn(IV) can be the main oxidiser of hydrogen sulfide. This form of Mn is being formed several meters higher than the sulfide onset via the reaction of dissolved manganese with oxygen. The precipitation of Mn(IV) leads to the increase of the particle's density

and acceleration of the rate of sinking (Yakushev, Debolskaya, 2001). Due to this, the depths of the sulfide onset and Mn(II) onset are different. With this model it is possible to demonstrate that the acceleration of sinking rate significantly affects one of the key features of the oxic/anoxic interface, the 5-10 m difference in depths between Mn(II) and sulfide onsets (Fig. 7A). In the absence of the accelerated rate of sinking of particles with settled Mn hydroxides (W_{Mn}=0) the oxic/anoxic interface shifted shallower, a H$_2$S onset was found at the same depth as Mn(II) onset, and a layer of co-existence of O$_2$ and H$_2$S appeared (Fig 7B).
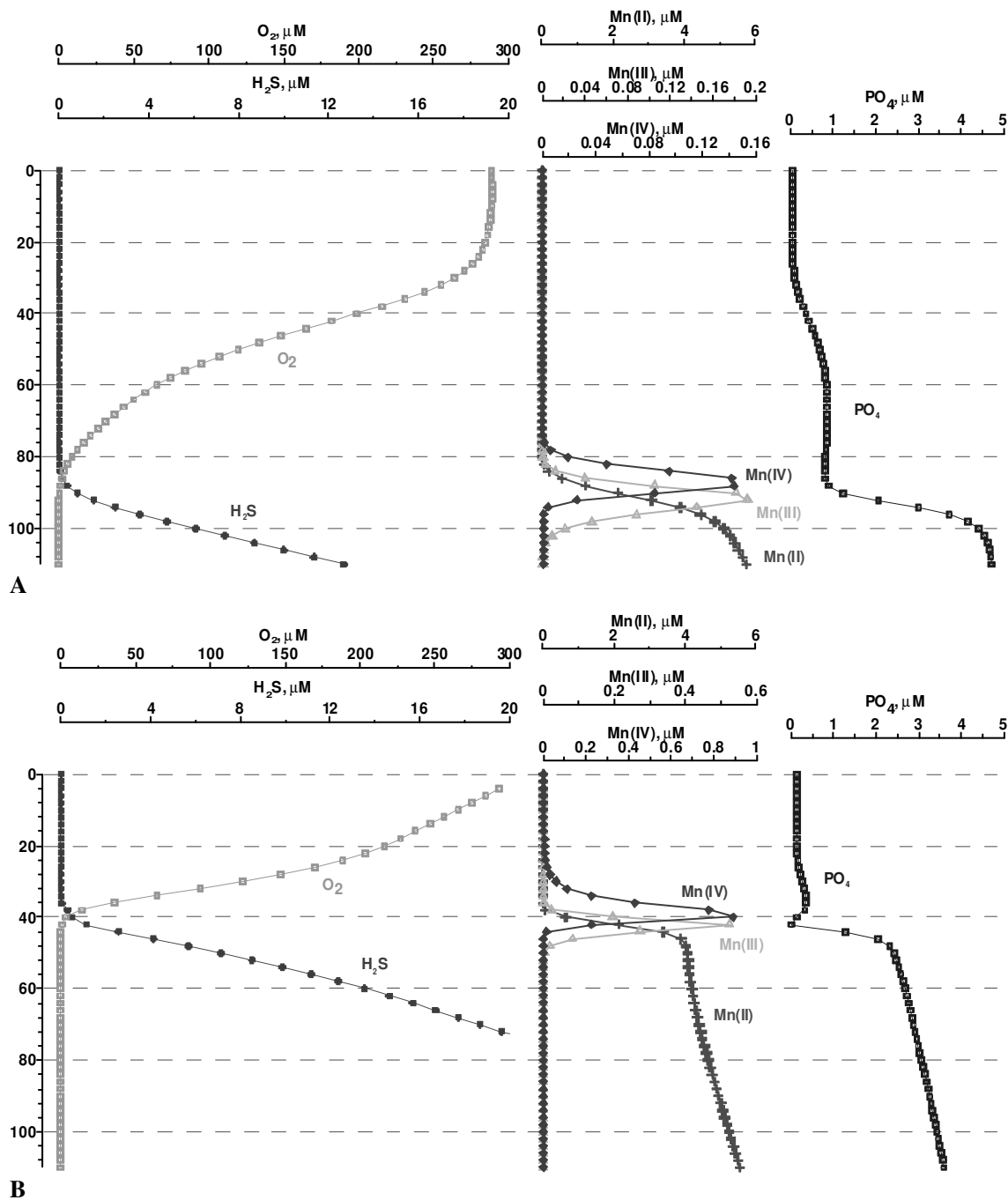

Fig. 7. Vertical distribution of O$_2$, H$_2$S, Mn(II), Mn(III), Mn(IV) and PO$_4$ in case accelerated rate of sinking of particles with settled Mn hydroxides W_{Mn}=18 m d^{-1} (A) and W_{Mn}=0 m d^{-1} (B).

This intense vertical transport of detrital particles with heavy manganese components is one reason for the existence of a zone with the absence of both significant concentrations of oxygen and sulfide, making possible such processes as anammox (Kuypers et al., 2003), reduction of Fe with Mn, and the presence of Mn in the form of Mn(III) (Trowburst et al., 2006) that is quickly oxidized in the presence of O_2 or reduced in the presence of H_2S (Webb et al., 2005).

7.2 Consumption of O_2 in the suboxic layer.

With this model we analyzed the roles of different processes on the O_2 consumption. The vertical distribution of these processes from the surface to the 200 m are presented in Fig. 8A. A dominant role in the oxygen consumption belongs to the processes of organic matter mineralization (49.2%) and respiration of living organisms (29.7%). These processes mainly compensate for the production of oxygen by photosynthesis. Nitrification consumes 10.8% of the oxygen in the lower part if the oxic zone. The share of oxidation of reduced compounds in the water column of a Sea with anoxic conditions can be estimates as less than 10%.
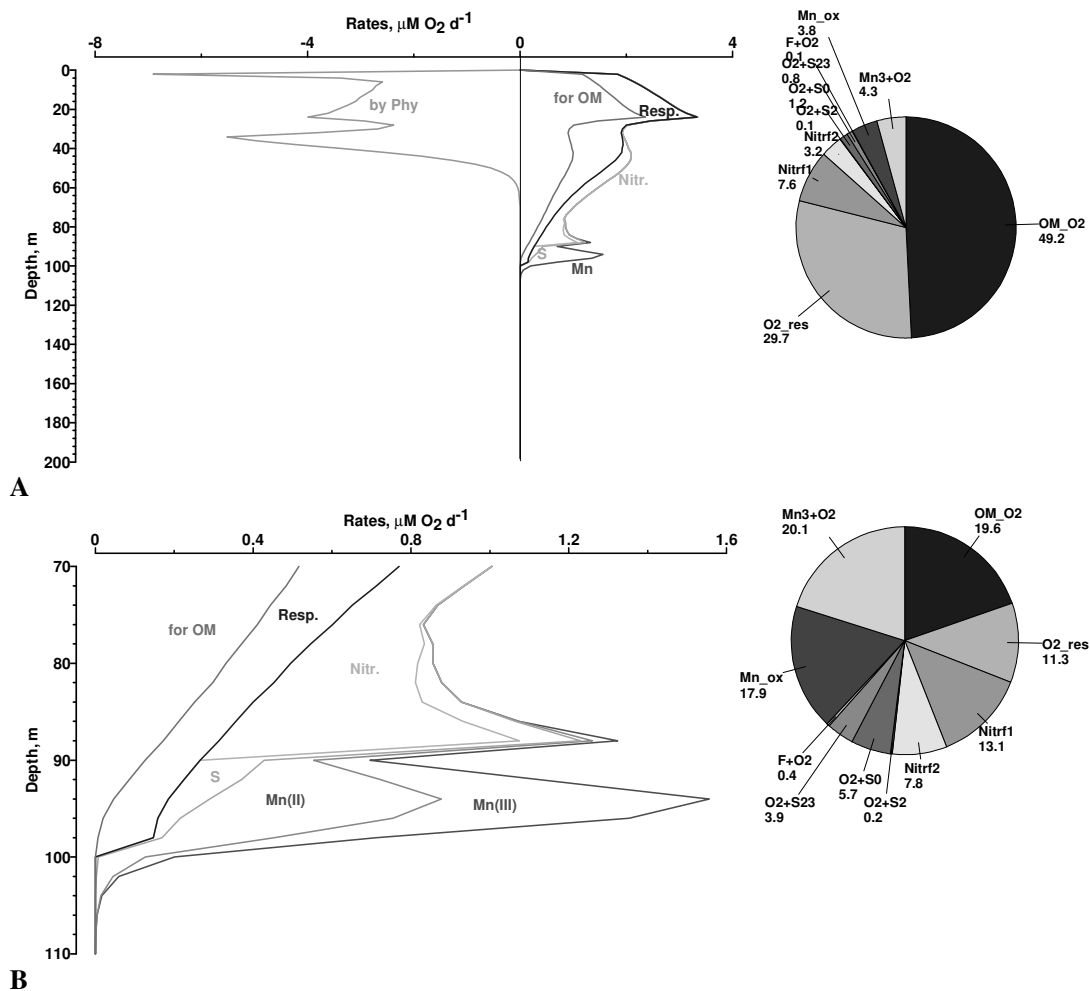

Fig. 8. Dissolved oxygen consumption in 0-200 m water column (A) and in the layer below 70 m (O_2<40 μM) (B).

Under oxygen-deficient conditions (from the concentrations of <40 μM to the sulfidic boundary, about (Fig. 8B), the share connected with the mineralization of OM and respiration was smaller (about 30%), because in this layer the decomposition of OM should be connected mainly with denitrification. The largest amount of O_2 was consumed by nitrification (mainly ammonia to nitrate oxidation – 13.1%, and amounts for nitrite to nitrate oxidation – 7.8%). Consumption for the oxidation of reductants was about 50 % (with a dominant share for Mn(III) (20.1%) and Mn(II) (17.9%) and less for reduced sulfur species). The amount of oxygen consumed for the oxidation of Fe(II) was negligible. Therefore the model numerically supports the ideas on the dominant role of the Mn cycle in the redox-interface structure of these systems.

These estimates appeared to be significant for the modification of ecological models. For example for studying of the large scale processes of oxygen depletion in the Baltic Sea with models (Fennel and Neumann, 2002; Savchuk, 2002; Gregoire et al., 1997) it will be possible to parameterize the dependence between the consumption of oxygen for supplied from anoxic zone ammonia oxidation and the consumption of oxygen for the oxidation of the other reductants (i.e. species of Mn, S, Fe). This model demonstrates that in the oxygen-deficient conditions the consumption of oxygen for oxidation of ammonia is approximately twice less than for oxidation of other reductants. This dependence can be easily added for the oxygen processes description in the ecological models that don't consider cycles of S, Mn and Fe.

7.3 "Phosphate dipole"

The vertical distribution of phosphate in the Black Sea is characterized by increased concentrations in the oxycline, a well pronounced shallow minimum about 5-10 m shallower than the sulfide onset, by a maximum below the sulfide onset, and by a second deep minimum about 30-50 m deeper (Fig. 2). This structure was called the "phosphate dipole" (Shaffer, 1986). The reason for formation of such a structure is still uncertain. Previously it was thought that it was connected with (1) chemosynthesis (Sorokin, 2002) and/or (2) phosphate co-precipitation with metal hydroxides (Shaffer, 1986). Both these theories probably are not correct, because (1) chemosynthesis has maximum values below the sulfide onset, where the phosphate content is also maximum, (2) co-precipitation with iron hydroxides should consume phosphate in ratio of 4:1.or 2.7:1 and the observing concentrations of iron hydroxides are very low (several tens of nM). Significant precipitation of phosphate with solid Mn(IV) has not been observed (Savenko and Baturin. 1996).

Recently, production of oxidized Mn in the form of Mn(III) has been observed by Mn(II)-oxidizing bacteria and in incubations with Black Sea suboxic zone water (Webb et al., 2005). Dissolved Mn(III) has also been directly observed in the suboxic zone in the SW Black Sea (Trowburst, et al., 2006). Mn(III) easily produces complexes with organic matter and pyrophosphate (Kostka et al., 1995). Pakhomova (2005) also suggested that Mn(II) to Mn(IV) oxidation goes through formation of complexes with manganese. Pyrophosphate particles were observed by T.Leipe (p.c., 2006) at the redox-interface of the Baltic Sea.
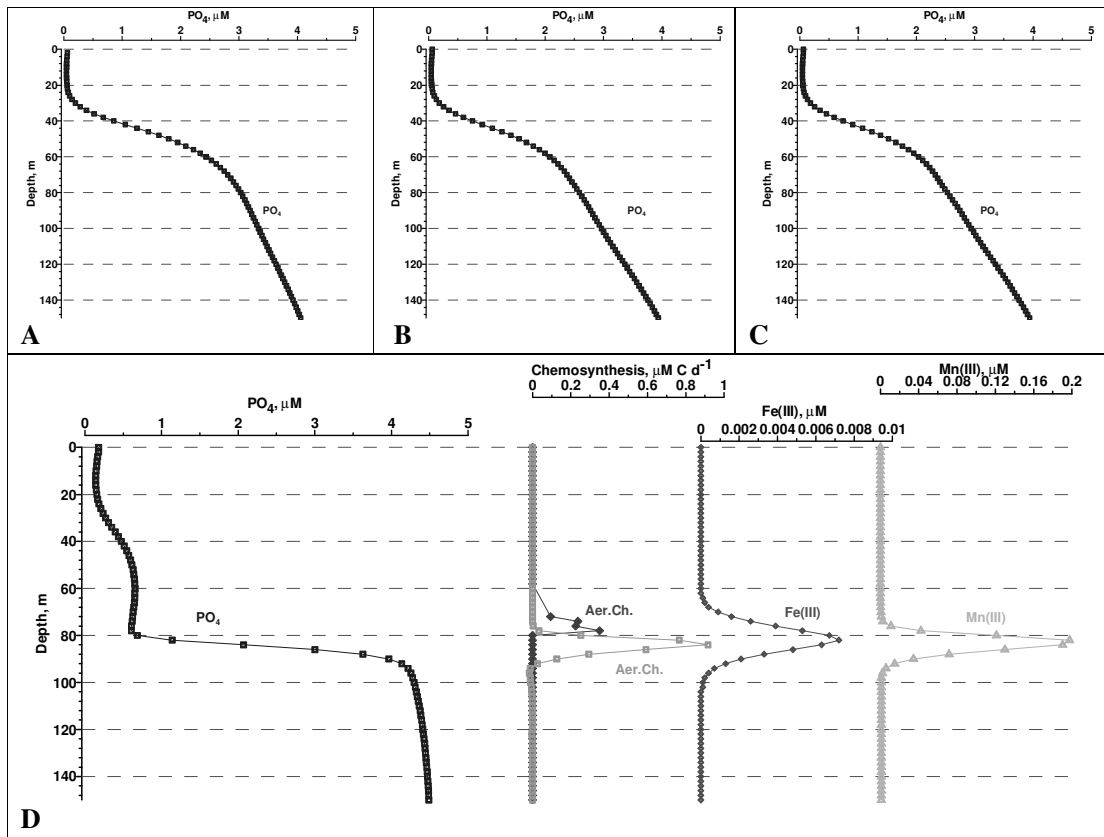
44

Fig. 9. Influence of chemosynthesis, co-precipitation with iron and manganese on the formation of "phosphate dipole". Explanations are in text.

The possible formation of Mn(III) complexes with pyrophosphate may explain this "phosphate dipole". The phosphorus minimum is located at the same depth, where Mn(II) depletes due to possible oxidation with oxygen, and its maximum is located about 5 m below the sulfide interface. We observed the maximum of polyphosphate in the same layer in the Northeastern Black Sea in 2006. These depths coincide with the likely limits of the Mn(III) maximum.

With this model we made a set of numerical experiments where we studied the influence of phosphate distribution on its consumption by (1) chemosynthesis, (2) co-precipitation with Fe(III) and (3) formation of complexes with Mn(III). The results are presented in Fig. 9.

In case of absence of all this factors the distribution of phosphate had no anomalies in the oxic/anoxic interface vicinity (Fig. 9A). Chemosynthesis resulted in negligible changes (Fig. 9B). Co-precipitation with Fe(III) with Fe/P=2.7 (T. Leipe, 2006, p.c.) leaded to some minor decrease in concentrations of phosphate (Fig. 9C), but the general shape of vertical distribution was far from the observed one (Fig. 2). Including the formation of complexes with Mn(III) with Mn/P=0.67 resulted in the formation of a vertical distribution that is very close to what we observed (Fig. 9D.). According to Davies (1969) the possible Mn(III) pyrophosphate complexes can have smaller values Mn/P=0.25 for $Mn(HP_2O_7)_2^{3-}$ or Mn/P =0.17 for $Mn(H_2P_2O_7)_3^{3-}$. The Mn(III) concentrations calculated by the this model were 0.2 μM (Fig. 8E) which were smaller than observed concentrations (0.5-1.5 μM, Trowburst et al., 2005). Therefore, it could be shown that the concentrations of Mn(III) could explain the phosphate dipole, even if Mn(III) only partly form complexes with P. Our studies in the Black Sea in September 2006 revealed a maximum of

polyphosphate (and pyrophosphate) in the depths of the phosphate dipole. Further study of the relations between Mn(III), pyrophosphate and polyphosphate are important for a better understanding the ecology of the Black Sea and the Baltic Sea, because the upward flux of phosphate limits in certain periods the photosynthesis.

7.4 Seasonal changes in the redox-layer.

The forcing of the seasonal variability on the differences in the redox layer structure was studied by this model with two scenarios – for the Black Sea and for the Baltic Sea.
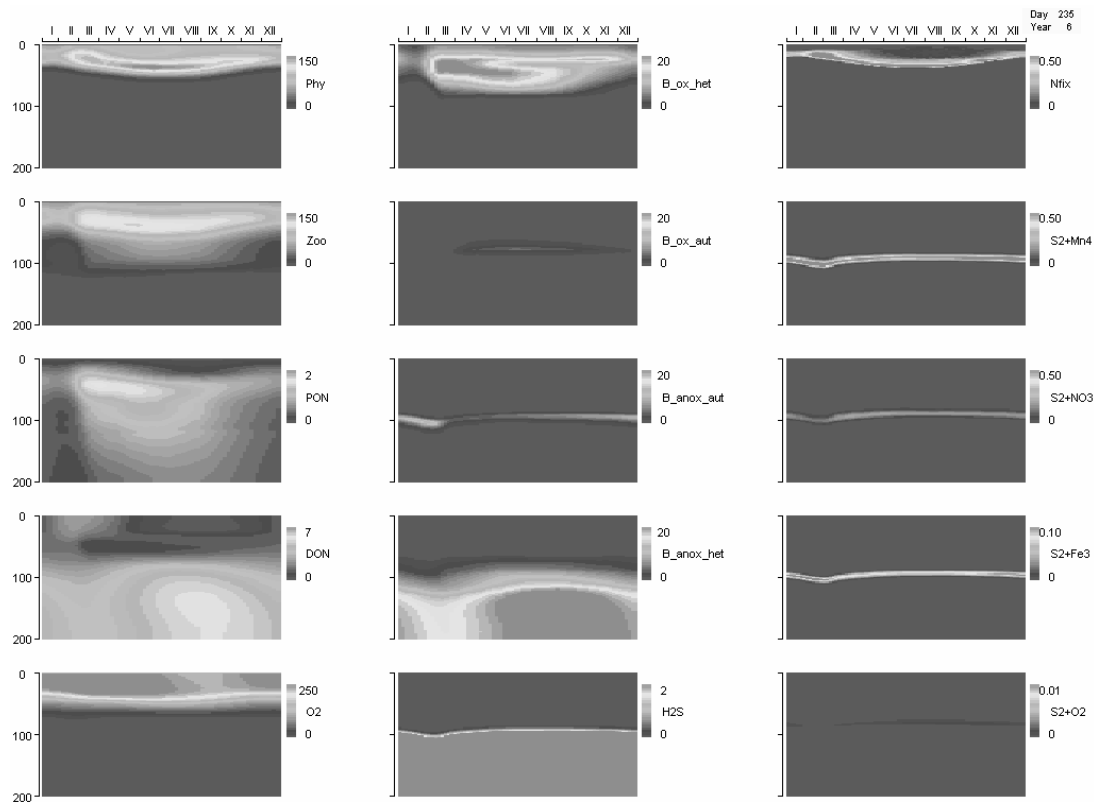
Fig. 10. Seasonal changes of vertical structure (Black Sea).

With a simplified scenario for the Black Sea (described above) it was shown that the seasonality of the phytoplankton development leads to increase of the flux of particulate organic matter to the anoxic zone. The oxygen content in the suboxic zone changed seasonally depending from the degradation of OM. (Fig. 10).

Calculations for the Baltic Sea were made on the basis of the results of GOTM model (Burchard et al., 1999). In this more realistic scenario the details of seasonal variability differed from the Black Sea: the spring bloom was more intense and shorter. In autumn, a second phytoplankton bloom was observed (Fig. 11). But as for the Black Sea, this numerical experiment reproduced the seasonal changes in the redox layer depths.

46
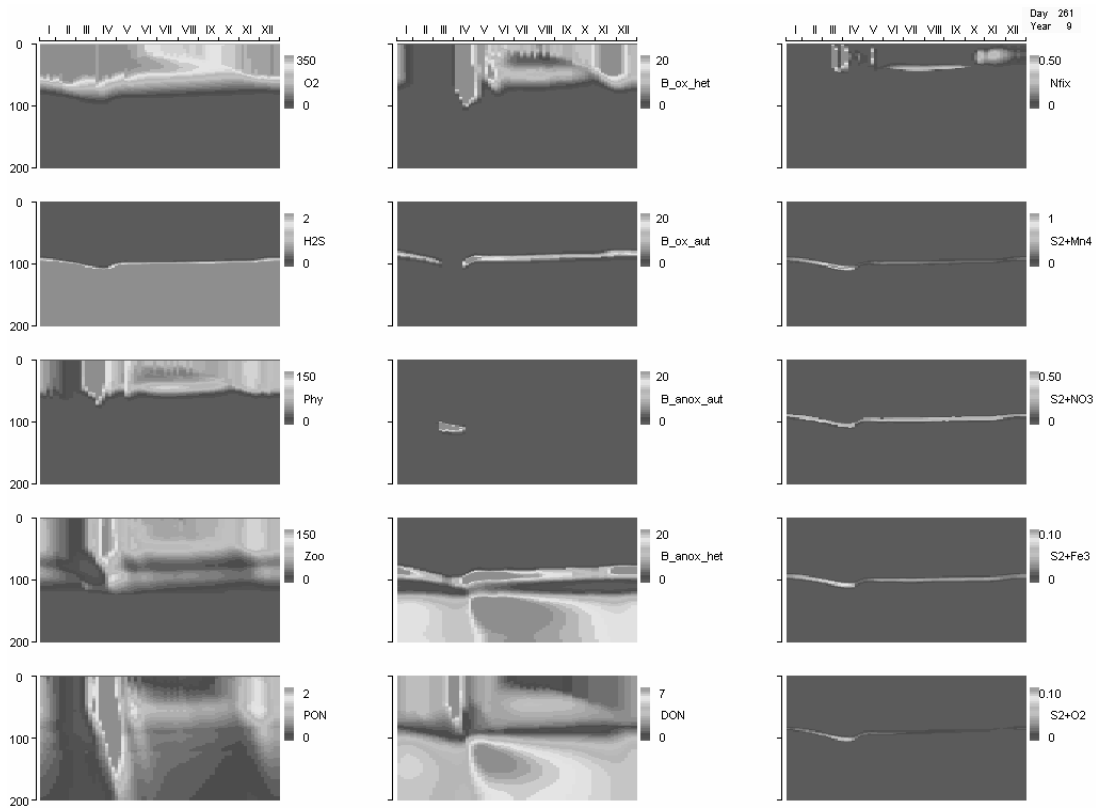
Fig. 11. Seasonal changes of vertical structure (Baltic Sea).

For both scenarios the calculations clearly show that the organic matter, formed in the euphotic layer, influences the structure and the processes in the redox-interface very significantly. There must be a competition for the dissolved oxygen between the particulate and dissolved organic matter supplied from the upper layers and reductants supplied from the anoxic zone (Fig. 12B,C).

As a result of this competition, mineralization of OM becomes more intense during summer. This process, is reflected also by the activity of heterotrophic bacteria (Fig. 10, 11, 12E,F) (both in oxic and anoxic zones) and also by the activity of aerobic autotrophic bacteria (nitrifiers). The activity of the anaerobic chemolithotrophic organisms was reduced in the warm period of the year (Fig. 10, 11, 12H), because lower concentrations of oxidants (probably metal hydroxides, which require oxygen for its formation) are available for anaerobic oxidation of sulfides and other reductants. After the end of the period of summer production of organic matter the activity of chemolithotrophic bacteria increases.
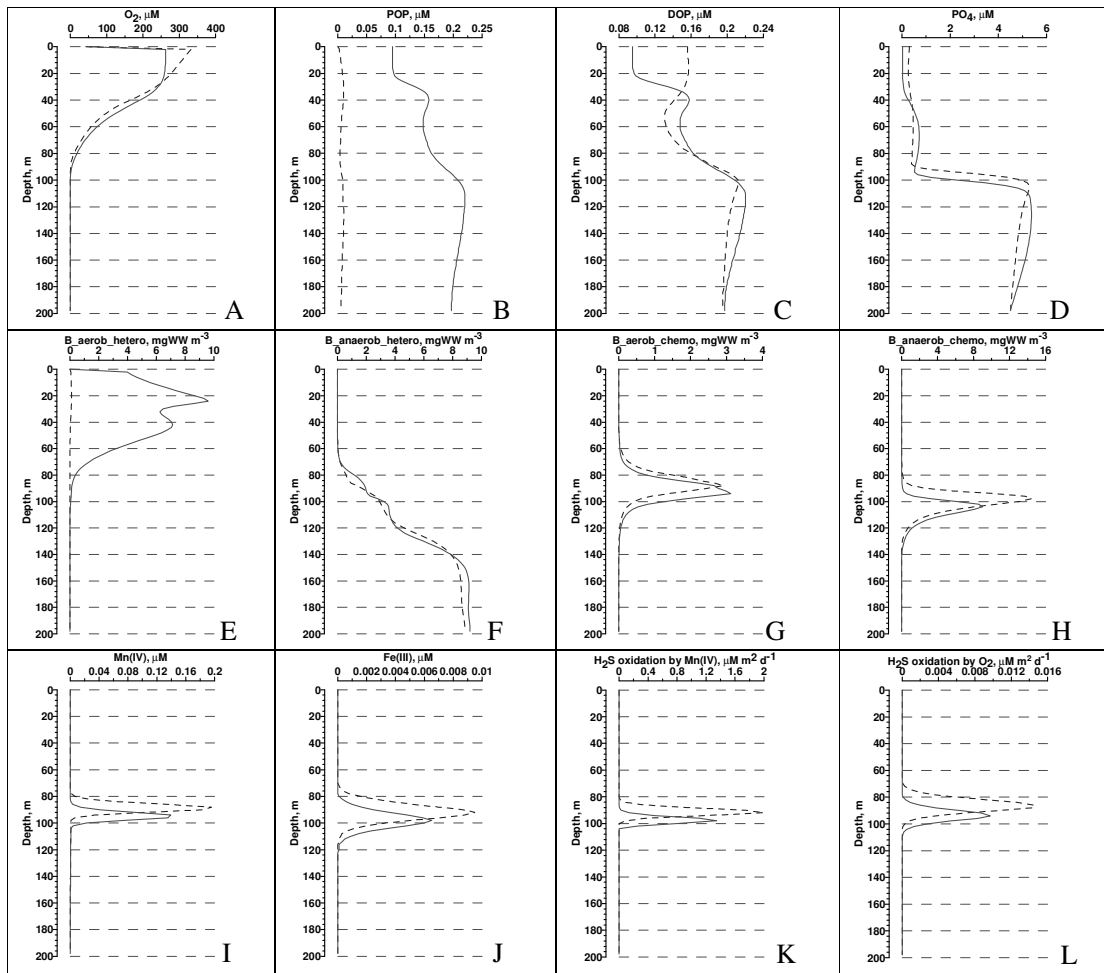
Fig. 12. Vertical distribution of *O2*, *POP*, *DOP*, *PO4*, aerobic heterotrophs, anaerobic heterotrophs, aerobic autotrophs, anaerobic autotrophs, *MnIV*, *FeIII*, *H2S* oxidation by *MnIV*, *H2S* oxidation by *O2*, in summer (solid line) and winter (dashed line).

Therefore, according to the model estimates, processes as ammonification, denitrification, sulfate reduction and nitrification are more intense in spring and summer of the year, while such processes as oxidation of reduced forms of metals, and of hydrogen sulfide (with all possible electron-acceptors) are more intense in the winter.

The model also showed that the shallow phosphate minimum was more pronounced in summer and practically absent in winter (Fig. 12D), corresponding to the observations (Yakushev et al., 2005).

The model demonstrates that in the seas with anoxic conditions N_2 fixation should occur. The large NO_3 losses by denitrification must be compensated in order to keep the system at a steady state with regard to dissolved inorganic nitrogen. In our calculations results, N_2 fixation should occur during the summer in the low boundary of the photic layer. (Fig. 9, 10). Many studies on N_2 fixation have been performed in the Baltic Sea and yielded a variety of contrasting estimates. This is partly due to different methodologies (Wasmund et al., 2005), but also reflects a pronounced interannual variability (Schneider et al., 2006). Recent investigations by Wasmund et al. (2005) and Schneider et al. (2002) indicate that the annual N_2 fixation may range between 120 and 300 mmol m^{-2} y^{-1},

48

respectively, and thus contribute up to 60 % of the annual nitrogen consumption in the central Baltic Sea surface water. The observations in the western Black Sea in August 2006 revealed intensive blooms of cyanobacteria (Mouncheva, 2006, p.c.) that confirm the results predicted with the model.

On the basis of this model it is possible to demonstrate the connection between the processes of biogeochemical transformations with the distribution of parameters and to distinguish 3 layers in the limits of redox zone:

7.5 Redox-layer structure.

7.5.1 Depth of NO3 maximum.

In the upper part of the redox-zone concentrations of dissolved oxygen decrease to 15-20 µM, and the vertical gradient of oxygen decreases and becomes equal to that of nitrate. Below this depth, nitrate, instead of oxygen, becomes the main electron acceptor for OM degradation. The reason for the decrease in the vertical gradient of oxygen is because there is a decrease in the consumption rates of oxygen for OM mineralization.

7.5.2 Depth of O2 depletion.

In the middle of the redox-zone, oxidized chemical compounds diffusing from the upper layer (oxygen and nitrate) decrease to zero (Yakushev et al., 2002; Stunzhas and Yakushev, 2006). This occurs simultaneously with the depletion of reductants ("deep" ammonia, manganese (II)), diffusing up from the anoxic zone. A minimum of phosphate is also found here. In the model, the redox reactions which deplete the remaining low oxygen concentrations result in disappearance/decrease of the mentioned reductants and the formation of alternative electron acceptors – respectively, particulate oxidized manganese (III,IV) and iron (III). In addition to diffusive transport they have a sinking rate that can accelerate the downward transport of these electron acceptors. A phosphate minimum could be mainly formed according its complexation with Mn(III). The role of other factors (co-precipitation with Fe and Mn oxids (Shaffer, 1986) and chemosynthesis (Sorokin, 2002)) is of less importance.

7.5.3 Depth of H2S onset.

The onset of hydrogen sulfide occurs just below the depths of peaks of oxidized Mn and Fe and corresponds to the lower part of the layer with the maximum phosphate gradient. The reduction of particulate manganese (IV) by sulfide is very intensive (Lewis and Landing, 1991; Rozanov, 1995) and model estimates (Yakushev and Debolskaya, 2000) suggest, that this reaction can be balanced by the hydrogen sulfide flux from below. A decrease of the PO4 vertical gradient or formation of the deep phosphate maximum occurs below the appearance of hydrogen sulfide because of degradation of its complexes with Mn(III).

The ability of this 1D model to reproduce the main basic features of the chemical structure of the central Black Sea and the Gotland Deep of the Baltic Sea suggests that the observed structures are formed by biogeochemical transformation and the processes included in the model. A role of lateral processes such as the influence of the Bosphorus plume in the Black Sea (Konovalov et al., 2003) should not be dominant in formation of the redox-layer structure.

8. Conclusions

We consider ROLM first of all as a tool for combined analysis of results from biological, chemical and physical observations. Being calibrated with observed data on the distribution of parameters, measured rates of processes and integrated estimates allows this tool to receive the numerical estimates on all the processes that influence the system under study.

- Seasonality of OM production results in (1) competition for the dissolved oxygen by reactions of mineralization of OM and by reactions of oxidizing reduced compounds (H_2S, NH_4, $Mn(II)$ and (2) in seasonality of the activity of the functional groups of bacteria involved in these processes. The heterotrophic processes should be more intense during the summer period and the development of heterotrophic aerobic and anaerobic bacteria as well as nitrifiers should be more pronounced. The chemolithotrophic bacteria connected with the intensity of the redox processes should be especially supported in winter.

- In the nitrogen balance of the Seas with anoxic conditions the intensity of denitrification is compensated by the N-fixation. Therefore, the development of anoxic zones should influence the intensity of N-fixation.

- The scenarios run by the model indicate that $Mn(III)$ may explain the phosphate dipole formation if it represents a large fraction of the dissolved Mn quantity in these depths. Study of the relationship between $Mn(III)$ and phosphate in the suboxic zone is critical for understanding the ecology and geochemistry of the Seas with anoxic conditions because photosynthesis can be limited by the upward flux of phosphate.

- The model offers the possibility that a layer with absence of both oxygen and hydrogen sulfide can exist in the redox zone (that, in particular, makes possible a reaction of anoxic oxidation of ammonia (anammox) (Kuypers et al., 2003) and allows Mn to exist in the water in the form of $Mn(III)$ (Trowburst and Luther, 2006). A dominant role in oxidation of the hydrogen sulfide at its onset level in this case should belong to the oxidized Mn compounds. H_2S oxidation occurs in the following shares due to reduction of $Mn(IV)$ – 50.2%, $Mn(III)$ – 42.6, NO_3 – 5.2%, $Fe(III)$ – 0.8 %, and O_2 - 1.1%.

- The role of iron cycling in the formation of the redox-layer structure is insignificant.

It is possible to conclude that the mathematical modelling of the redox systems is a useful tool for revealing the gaps in knowledge and the perspective directions of studies and for the analysis of reaction of the redox systems on natural and anthropogenic forcing.

References

Ali K. and Ashiq U. (2004): Study of the kinetics and activation parameters of reduction of Mn(III) to Mn(II) by SO_3^{2-} ion in $(MnSiW_{11}O_{40}H_2)^{5-}$ heteropoly ion. - J.of Iran. Chem. Soc., 1(2), 122-127.

Anderson, J.J., Okubo A., Robbins A.S. and Richards F.A. (1982): A model for nitrite and nitrate distributions in oceanic oxygen minimum zones. - Deep-Sea Res., 29, 1113-1140.

Ayzatulllin T.A. and Leonov A.V. (1975): Kinetics and mechanism of the oxidizing transformation of anoxic sulfur compounds in the sea water. - Okeanologiya, V. 15, No 6, 1026-1033. (in Russian).

Bauer S. (2003): Structure and function of nitrifying bacterial communities in the eastern Gotland basin (central Baltic Sea). - Mathematisch-Naturwissenschaftliche Fakultat. Univesitat Rostock, Rostock, 120.

Boudreau B.P. (1996): A method-of lines code for carbon and nutrient diagenesis in aquatic sediments. - Computers & Geosciences., V. 22, No 5, 479-496.

Brettar I. and Rheinheimer G. (1991): Denitrification in the Central Baltic: evidence for H2S-oxidation as motor of denitrification at the oxic-anoxic interface. - Marine Ecology Progress Series, 77(2-3), 157-169.

Burchard H., Bolding K. and Villareal M.R. (1999): GOTM, a general ocean turbulence model. Theory, applications and test cases. - European Commission report EUR 18745 EN, 103.

Canfield D.E., Thamdrup B. and Kristensen E.(2005): Aquatic geomicrobiology. - In: Southward A.J., Tyler P.A., Young C.M. and Fuiman L.A. (Ser. Editors): Advances in Marine Biology, 48, Elsevier Acad. Press., Amsterdam - Tokio, 640.

Dalsgaard T., Canfield D.E., Peterson J., Thamdrup B., Acuna-Gonzalez J. (2003) N_2 production by the anammox reaction in the anoxic water column of Golfo Dolce, Costa Rica. –Letters to Nature, 422, 606-608.

Davis G. (1969): Some aspects of chemistry of Mn(III) in aqueous solutions. - Coord. Chem. Rev., 4, 199-224.

Dollhopf M.E., Nealson K.H., Simon D.M. and Luther III G.W. (2000) Kinetics of Fe(III) and MN(IV) reduction by the Black Sea strain of Schewanella Putrefaciens using in situ solid state voltammetric AU/Hg electrodes. - Marine Chemistry, 70, 171-180.

Enoksson V. (1986): Nitrification rates in the Baltic Sea: Comparison of tree isotope techniques. - Applied and Environmental Microbiology, 51(2), 244-250.

Erdogan S., Yemenicioglu S. and Tugrul S. (2003): Distribution of dissolved and particulate forms of iron and manganese in the Black Sea. - In: A. Yilmaz (Ed.): Oceanography of the Eastern Mediterranean and Black Sea. - Tubitak Publishers, Ankara, 447-451.

Fasham M.J., Ducklow H.W. and McKelvie S.M. (1990): A nitrogen-based model of plankton dynamics in the oceanic mixed layer. - J. Mar. Res., 48, 591-639.

Feistel R., Nausch G., Matthaus W. and Hagen E. (2003): Temporal and spatial evolution of the Baltis deep water renewal in spring 2003. - Oceanologia, 45 (4), 623-642.

Fennel W. and Neumann T. (2004) Introduction to the modeling of marine ecosystems. - In: D.Halpne (Ed.): Elsevier Oceanography, 72, 298.

Fonselius S.H. (1974): Phosphorus in the Black Sea. - In: Degens E.J. and Koss D.A. (Editors): The Black Sea – Geology, Chemistry and Biology. Amer. Ass. of Petrol. Geologists, Tusla, 144-150.

Gargett A.E. (1984) Vertical eddy diffusivity in the ocean interior. - J. of Marine Res, 42, 359-393.

Gregoire M., Beckers J.-M., Nihoul J.C.J. and Stanev E. (1997): Coupled hydrodynamic ecosystem model of the Black Sea at basin scale. - In: Ozsoy E. and Mikaelyan A. (Editors): Sensitivity to Change: Black Sea, Baltic Sea and North Sea. Netherlands, Kluwer, 487-499.

Hannig M., Lavik G., Kuypers M., Wobken D. and Jurgens K. (2006): Distribution of denitrification and anammox activity in the water column of the central Baltic Sea. - 9th Int. Estuarine Biogeochemistry Symposium. Estuaries and Enclosed Seas under Changing Environmental Conditions. May 7-11, 2006, Warnemuende, Germany, 49.

HELCOM (2002): Environment of the Baltic Sea area 1994-1998. - Balt. Sea Environ. Proceedings No 82B., 216.

Konovalov S.K., Luther G.W., Friederich G.E., Nuzzio D.B., Tebo B.M., Oguz T., Glazer B., Trouwborst R.E., Clement B., Murray K.J. and Romanov A.S. (2003): Lateral injection of oxygen with Bosporus plume – fingers of oxidizing potential in the Black Sea. - Limnol. Oceanogr., 48(6), 2367-2376.

Konovalov S.K., Murray J.W., Luther G.W. and Tebo B.M. (2006): Processes controlling the Redox budget for oxic/anoxic water column of the Black Sea. - Deep Sea (II), doi:10.1016/j.dsr2.2006.03.013..

Kostka, J. E., Luther III G. W. and Nealson K. H. (1995): Chemical and biological reduction of Mn(III)-pyrophosphate complexes: potential importance of dissolved Mn(III) as an environmental oxidant. - Geochim. Cosmochim. Acta 59, 85-894.

Kuypers M.M.M., Sliekers A.O, Lavik G., Schmid M., Jorgensen B.B., Kuenen J.G., Sinnenghe Damste J.S., Strous M. and Jetten M.S.M. (2003): Anaerobic ammonium oxidation by anammox bacteria in the Black Sea. - Nature, 422, 608-611.

Lewis B.L. and Landing W.M. (1991): The biogeochemistry of manganese and iron in the Black Sea. Deep Sea Res., 38(2A), S773-S803.

Lipschultz F., Wofsy S.C., Ward B.B., Codispoti L.A., Friederich G. and Elkins J.W. (1990): Bacterial transformations of inorganic nitrogen in the oxygen-deficient waters of the eastern tropical South Pacific Ocean - Deep Sea Res., 37, 1513-1541.

Murray, J.W., Codispoti L.A. and Friederich G.E. (1995): The suboxic zone in the Black Sea - In: Huang C.P., O'Melia R. and Morgan J.J. (Editors): Aquatic chemistry: interfacial and interspecies processes, American Chemical Society, 157-176.

Murray J. W. and Yakushev E. V. (2006): The suboxic transition zone in the Black Sea. - In: L.N. Neretin (Ed.): Past and Present Water Column Anoxia. NATO Sciences Series, Springer., 105-138.

Nealson K.H., Myers C.R. and Wimpee B.B. (1991): Isolation and identification of manganese reducing bacteria and estimates of microbial Mn (IV)-reducing potential in the Black Sea. - Deep-Sea Res., 38, S907-S920.

Nealson K.N. and Stahl D.A. (1997): Microorganisms and biogeochemical cycles: what can be learn from layered microbial communities? - In: Banfield J.F. and Nealson K.N. (Editors): Geomicrobiology: Interactions between Microbes and Minerals,. Reviews in mineralogy, V. 35, Washington D.C. Mineralogical Society of America., 5-34.

Neretin L., Pohl, C., Jost G., Leipe T. and Pollehne F. (2003): Manganese cycling at the oxic/anoxic interface in the Gotland deep, Baltic Sea. - Marine Chemistry, 82, 125-143.

Oguz T., Ducklow H., Shushkina E.A., Malonotte-Rizzoli P., Tugrul S. and Lebedeva L.P. (1998): Simulation of upper layer biochemical structure in the Black Sea. - In: L.Ivanov and Oguz T. (Editors): NATO TU-Black Sea Project. Ecosystem Modeling as a Tool for the Black Sea, Symposium on Scientific Results, Kluwer Academic Publishers, V.2., 257-299.

Overmann J. and Manske A.K. (2005): Anoxygenic phototrophic bacteria in the Blcak Sea chemocline. - In: Neretin L.N. (Ed.): Past and Present Water Column Anoxia. NATO Sciences Series, Springer., 501-522.

Pakhomova S.V. (2005): Dissolved forms of iron and manganese in marine water, sediments and the water-bottom boundary. - Ph.D.Thesis., SIO RAS, Moscow, 24.

Pimenov N.G. and Neretin L.N. (2006): Composition and activities of microbial communities, involved in carbon, sulfur, nitrogen and manganese cycling in the oxic/anoxic interface of the

Black Sea. - In: Neretin L.N. (Ed.): Past and Present Water Column Anoxia. NATO Sciences Series, Springer., 501-522.

Richards F.A. (1965): Anoxic basins and fjords. - In: Riley J.P. and Skirrow G. (Editors): Chemical Oceanography, 1, Academic Press, NY, 611-645.

Richardson K. and Jorgenson B.B. (1996) : Eutrophication: Definition, History and Effects. - In: Jorgenson B.B. and Richardson K. (Editors): Eutrophication in Coastal Marine Ecosystems. Coastal and Estuarian Studies, 52. AGU, Washington D.C., 1-19.

Richardson L.L., Aguilar C. and Nealson K.H. (1988): Manganeses oxidation in pH and O2 microenvironments produced by phytoplankton. - Limnol. Oceanogr., 33(3), 352-363.

Rozanov, A.G. (1995): Redox stratification of the Black Sea water. - Oceanology 35, 544-549.

Samodurov A.S. and Ivanov L.I. (1998): Processes of Ventilation of the Black Sea Related to Water Exchange through the Bosphorus. - NATO ASI Series. NATO TU Black Sea Project. Ecosystem Modeling as a Management Tool for the Black Sea. Symp. on Sci. Res. Kluwer Ac. Pub., Netherland, V. 2/47(2). P.II ., 221-236.

Savchuk O. and Wulff F. (1996): Biogeochemical Transformation of nitrogen and phosphorus in the marine environment. Coupling hydrodynamic and biogeochemical processes in models for the Baltic proper. - Systems ecology contributions No 2. Stockholm University, Stockholm, 79.

Savchuk O. (2002): Nutrient biogeochemical cycles in the Gulf of Riga: scaling up field studies with a mathematical model. - Journal of Marine Systems, 32, 253-280.

Savenko A. V. (1995): Precipitation of phosphate with iron hydroxide forming by mixing of submarine hydrothermal solutions and the sea water (on the base of experimental data). - Geochemistry International., 9, 1383-1389.

Savenko A.V. and Baturin G.N. (1996): Experimental study of the sorption of phosphorus on manganese dioxide. - Geochemistry, 5, 472-474.

Schneider B., Nausch G., Kubsch H. and Peterson I. (2002): Accumulation of total CO2 during stagnation in the Baltic deep water and its relationship to nutrient and oxygen concentrations. - Marine Chemistry, 77, 277-291.

Scranton M.I., McIntyre M., Astor Y., Taylor G.T., Muller-Karger F. and Fanning K. (2006): Temporal variability in the nutrient chemistry of the Cariaco basin. - In: Neretin L.N. (Ed.): Past and Present Water Column Anoxia. - NATO Sciences Series, Springer., 105-138.

Sergeev, Y. N. (Ed.), (1979): Modelirovaniye Perenosa i Transformatsii Veshchestv v More (Modeling of Transport and Transformation of Substances in the Sea), Leningrad State Univ., St. Petersburg, Russia, 296. (in Russian).

Shaffer G. (1986): Phosphorus pumps and shuttles in the Black Sea. - Letters to Nature, Nature, 321, 515-517.

Sorokin Yu.I. (1962): Eksperimentalnye issledovaniya sulfatreduktsii v Chyorno more s ispolzovaniem [35]S (Experimantal investigation of sulfate reduction in the Black Sea by use of ^{35}S). - Mikrobiologiya, 3, 402-410. (in Russian).

Sorokin Yu.I., Sorokin D.Yu. and Avdeev V.A. (1991) Aktivnost' mikroflory i okislitel'nye protsessy sernogo tsykla v tolshche vody Chernogo morya (Microbial activity and sulfur cycle oxidation processes in the Black Sea water column). - In: Vinogradov M. (Ed.): Izmenchivost' Ekosystemy Chernogo Morya (Estesstvennye i Antropogennyye Faktory), Nauka, Moscow, 173-188. (in Russian)

Sorokin Yu.I. (1992): Raspredeleniye i funktsional'naya aktivnost' mikroflory v tolshche vody Chernogo morya zimoy i v nachale vesny 1991 g. (Distribution and functional activity of microflora in the Black Sea water column during winter and early spring 1991). - In: M.Vinogradov (Ed.): *Zimnee Sostoyaniye Ekosystemy Otkrytoy Chasti Chernogo Morya*, P.P.Shirshov Inst. of Oceanol., Russ. Acad. of Sci., Moscow, 89-102. (in Russian)

Sorokin Yu.I. (2002): The Black Sea. Ecology and Oceanography. - Backhuys Publishers, Leiden, 875.

Stal L.J. and Walsby A.E. (2000): Photosynthesis and nitrogen fixation in a cyanobacterial bloom in the Baltic Sea. - European Journal of Phycology, 35(2), 97-108.

Steele J.H., Frost B.W. (1977): The structure of plankton communities - Phil. Trans. Roy. London A. 280, 485-534.

Stokozov N. A. (2004): Long-lived radionuclides ^{137}Cs and ^{90}Sr in the Black Sea after the Chernobyl NPP accident and their use as a tracers of water exchange processes. - Ph.D.Thesis., MHI, Sebastopol, 21.

Stunzhas P.A. (2000): On the structure of the zone of interactions of the aerobic and anaerobic waters of the Black Sea of the basis of measurements with an membrane-free sensor of oxygen. - Oceanology, 40(4), 503-509.

Stunzhas P.A. and Yakushev E.V. (2006): On the Black Sea redox-zone fine chemical structure of the base of measurements with an oxygen open sensor and Niskin bottles sampling. - Okeanologiya, 46(5), 665-677. (in Russian)

Tebo B.M. (1991): Manganese (II) oxidation in the suboxic zone of the Black Sea. - Deep Sea Res., 38, S883-S906.

Tebo B.M., Ghiorse W.C., van Waasbergen V.G., Siering P.L. and Caspi L. (1997): Bacterially mediated mineral foundation: Insights into manganese (II) oxidation from molecular genetic and biochemical studies - In: Banfield J.F. and Nealson K.H. (Editors): Reviews in Mineralogy, Vol. 35, Geomicrobiology Interactions berween Microbs and Minerals. Mineralogical Society of America, Washington DC., 225-266.

Thamdrup B. (1997) Bacterial manganese and iron reduction in aquatic sediments. – Advances in Microbiobial Ecology, V.16, Bernhard Schrink (ed.), 41-84.

Trouwborst R.E., Clement B.G., Tebo B.M., Glazer B.T., and Luther III G.M. (2006): Soluble Mn(III) in suboxic zones – Science, 313(5795), 1955-1957.

UNESCO (1986): Progress on oceanographic tables and standards 1983-1986 : work and recommendations of the UNESCO/SCOR/ICES/IAPSO Joint Panel.- Unesco Technical papers in marine science, ndeg. 50, 59.

Volkov I.I. (1974): Geokhimiya sery v osadkah okeana (Geochemistry of sulfur in the ocean sediments). - Nauka, Moscow, 272. (In Russian).

Volkov I.I., Rozanov A.G. and Demidova T.P. (1992): Reduced inorganic sulfur species and dissolved manganese in the water of the Black Sea. - In: Vinogradov M.E. (Ed.): Winter state of the ecosystem of the open part of the Black Sea. Shirshov Institute of Oceanology RAS, Moscow, 38-50.

Wanninkhof R. (1992): Relationship between Wind Speed and Gas exchange over the Ocean. - J.Geophys.Res., v.97, No C5, 7373-7382.

Ward B.B. and Kilpatrick K.A. (1991): Nitrogen transformations in the oxic layer of permanent anoxic basins: The Black Sea and the Cariaco Trench, in Black Sea Oceanography. - In: Izdar E. and Murray J.W. (Editors): Kluwer Acad., Norwell, Mass., 111-124.

Wasmund N., Andrushaitis A., Lsiak-Pastuszak E., Muller-Karulis B., Nausch G., Neumann T., Ojaveer H., Olenina I., Postel L. and Witek Z. (2001): Trophic status of the southeastern Baltic Sea: a comparison of coastal and open areas. – Estuarine, Coastal and Shelf Science. 56, 849-864.

Wasmund N., Nausch G. et al. (2005): Comparison of nitrogen fixation rates determined with different methods: a study in the Baltic Proper. - Marine Ecology Progress Series 297, 23-31.

Webb S.M., Dick G.J., Bargar J.R. and Tebo B.M. (2005): Evidence for the presence of Mn(III) intermediates in the bacterial oxidation of Mn(II). - In Fridovich I. (Ed.), PNAS, Vol. 102, No. 15, 5558-5563.

Yakushev E.V. (1992): Numerical modeling of transformation of nitrogen compounds in the redox zone of the Black Sea. - Oceanology, Vol.32, No 2, 173-177.

Yakushev E.V. and Mikhailovsky G.E (1995): Mathematical modeling of the influence of marine biota on the carbon dioxide ocean-atmosphere exchange in high latitudes. - In: Jaehne B. and Monahan E. C. (Editors): Air-Water Gas Transfer, Sel. Papers, Third Int. Symp., July 24-27, Heidelberg University, AEON Verlag & Studio, Hanau , 37–48.

Yakushev E.V. and Neretin L.N. (1997): One-Dimensional Modeling of Nitrogen and Sulfur Cycles in the Aphotic Zones of the Black and Arabian Seas. - Global Biogeochemical Cycles, Vol. 11, No 3, 401-414.

Yakushev E.V. (1999): An approach to modelling anoxic conditions in the Black Sea. Environmental degradation of the Black Sea: Challenges and Remedies. - Kluwer Academic Publishers, 93-108.

Yakushev E.V. and Debolskaya E.I. (2000): Particulate manganese as a main factor of oxidation of hydrogen sulfide in redox zone of the Black Sea. - Proc. Konstantin Fedorov Memorial Symposium. Oceanic Fronts and Related Phenomena 18 - 22 May, 1998. Pushkin, Saint-Petersburg, Russia.. IOC Workshop Report No. 159, Kluwer Academic Publishers, 592-597.

Yakushev E.V., Lukashev Yu.F., Chasovnikov V.K. and Chzhu V.P. (2002): Modern notion of the vertical hydrochemical structure of the Black Sea redox zone. - In: Zatsepin A.G. and Flint M.V. (Editors): Complex investigation of the Northeastern Black Sea. - Nauka, Moscow, 119-133. (In Russian).

Yakushev E.V., Chasovnikov V.K., Debolskaya E.I., Egorov A.V., Makkaveev P.N., Pakhomova S.V., Podymov O.I. and Yakubenko V.G. (2006): The northeastern Black Sea redox zone: hydrochemical structure and its temporal variability. - Deep Sea Research II, 53, 1764-1786.

Yao W. and Millero F. (1996): Adsorption of Phosphate on Manganese Dioxide in Seawater. - Environ. Sci. Technol., 30, 536-541.

Yilmaz, A., Coban-Yildiz Y., Telli-Karakoc F. and Bologa A. (2006): Surface and mid-water sources of organic carbon by photo- and chemoautotrophic production in the Black Sea. - Submitted to Deep Sea Research Part II, Special Issue. (accepted).

Zehr J.P., Church M.J. and Moisander P.H. (2006): Diversity, distribution and biochemical significance of nitrogen-fixing organisms in anoxic and suboxic environments. - In: Neretin L.N. (Editor): Past and Present Water Column Anoxia. NATO Sciences Series, Springer., 337-369.

Zopfi J., Ferdelman T.G., Jorgensen B.B., Teske A. and Thamdrup B. (2001): Influence of water column dynamics on sulfide oxidation and other major biogeochemical processes in the chemocline of Mariager Fjord (Denmark). - Marine Chemistry., 74, 29-51.

Meereswissenschaftliche Berichte
MARINE SCIENCE REPORTS

1 (1990)   Postel, Lutz:
        Die Reaktion des Mesozooplanktons, speziell der Biomasse, auf küstennahen Auftrieb vor Westafrika (The mesozooplankton response to coastal upwelling off West Africa with particular regard to biomass)

2 (1990)   Nehring, Dietwart:
        Die hydrographisch–chemischen Bedingungen in der westlichen und zentralen Ostsee von 1979 bis 1988 – ein Vergleich (Hydrographic and chemical conditions in the western and central Baltic Sea from 1979 to 1988 – a comparison)
        Nehring, Dietwart; Matthäus, Wolfgang:
        Aktuelle Trends hydrographischer und chemischer Parameter in der Ostsee, 1958 – 1989 (Topical trends of hydrographic and chemical parameters in the Baltic Sea, 1958 – 1989)

3 (1990)   Zahn, Wolfgang:
        Zur numerischen Vorticityanalyse mesoskaler Strom- und Massenfelder im Ozean (On numerical vorticity analysis of mesoscale current and mass fields in the ocean)

4 (1992)   Lemke, Wolfram; Lange, Dieter; Endler, Rudolf (Eds.):
        Proceedings of the Second Marine Geological Conference – The Baltic, held in Rostock from October 21 to October 26, 1991

5 (1993)   Endler, Rudolf; Lackschewitz, Klas (Eds.):
        Cruise Report RV "Sonne" Cruise SO82, 1992

6 (1993)   Kulik, Dmitri A.; Harff, Jan:
        Physicochemical modeling of the Baltic Sea water–sediment column: I. Reference ion association models of normative seawater and of Baltic brackish waters at salinities 1–40 ‰, 1 bar total pressure and 0 to 30 C temperature
        (system Na–Mg–Ca–K–Sr–Li–Rb–Cl–S–C–Br–F–B–N–Si– P–H–O)

7 (1994)   Nehring, Dietwart; Matthäus, Wolfgang; Lass, Hans Ulrich; Nausch, Günther:
        Hydrographisch–chemische Zustandseinschätzung der Ostsee 1993

8 (1995)   Hagen, Eberhard; John, Hans-Christian:
        Hydrographische Schnitte im Ostrandstromsystem vor Portugal und Marokko 1991 - 1992

9 (1995)   Nehring, Dietwart; Matthäus,Wolfgang; Lass, Hans Ulrich; Nausch, Günther; Nagel, Klaus:
        Hydrographisch-chemische Zustandseinschätzung der Ostsee 1994
        Seifert, Torsten; Kayser, Bernd:
        A high resolution spherical grid topography of the Baltic Sea

10 (1995)   Schmidt, Martin:
        Analytical theory and numerical experiments to the forcing of flow at isolated topographic features

11 (1995)   Kaiser, Wolfgang; Nehring, Dietwart; Breuel, Günter; Wasmund, Norbert; Siegel, Herbert; Witt, Gesine; Kerstan, Eberhard; Sadkowiak, Birgit:
        Zeitreihen hydrographischer, chemischer und biologischer Variablen an der Küstenstation Warnemünde (westliche Ostsee)
        Schneider, Bernd; Pohl, Christa:

		Spurenmetallkonzentrationen vor der Küste Mecklenburg-Vorpommerns
12	(1996)	Schinke, Holger: Zu den Ursachen von Salzwassereinbrüchen in die Ostsee
13	(1996)	Meyer-Harms, Bettina: Ernährungsstrategie calanoider Copepoden in zwei unterschiedlich trophierten Seegebieten der Ostsee (Pommernbucht, Gotlandsee)
14	(1996)	Reckermann, Marcus: Ultraphytoplankton and protozoan communities and their interactions in different marine pelagic ecosystems (Arabian Sea and Baltic Sea)
15	(1996)	Kerstan, Eberhard: Untersuchung der Verteilungsmuster von Kohlenhydraten in der Ostsee unter Berücksichtigung produktionsbiologischer Meßgrößen
16	(1996)	Nehring, Dietwart; Matthäus, Wolfgang; Lass, Hans Ulrich; Nausch, Günther; Nagel, Klaus: Hydrographisch-chemische Zustandseinschätzung der Ostsee 1995
17	(1996)	Brosin, Hans-Jürgen: Zur Geschichte der Meeresforschung in der DDR
18	(1996)	Kube, Jan: The ecology of macrozoobenthos and sea ducks in the Pomeranian Bay
19	(1996)	Hagen, Eberhard (Editor): GOBEX - Summary Report
20	(1996)	Harms, Andreas: Die bodennahe Trübezone der Mecklenburger Bucht unter besonderer Betrachtung der Stoffdynamik bei Schwermetallen
21	(1997)	Zülicke, Christoph; Hagen, Eberhard: GOBEX Report - Hydrographic Data at IOW
22	(1997)	Lindow, Helma: Experimentelle Simulationen windangeregter dynamischer Muster in hochauflösenden numerischen Modellen
23	(1997)	Thomas, Helmuth: Anorganischer Kohlenstoff im Oberflächenwasser der Ostsee
24	(1997)	Matthäus, Wolfgang; Nehring, Dietwart; Lass, Hans Ulrich; Nausch, Günther; Nagel, Klaus; Siegel, Herbert: Hydrographisch-chemische Zustandseinschätzung der Ostsee 1996
25	(1997)	v. Bodungen, Bodo; Hentzsch, Barbara (Herausgeber): Neue Forschungslandschaften und Perspektiven der Meeres-forschung - Reden und Vorträge zum Festakt und Symposium am 3. März 1997.
26	(1997)	Lakaschus, Sönke: Konzentrationen und Depositionen atmosphärischer Spurenmetalle an der Küstenstation Arkona
27	(1997)	Löffler, Annekatrin: Die Bedeutung von Partikeln für die Spurenmetallverteilung in der Ostsee, insbesondere unter dem Einfluß sich ändernder Redoxbedingungen in den zentralen Tiefenbecken
28	(1998)	Leipe, Thomas; Eidam, Jürgen; Lampe, Reinhard; Meyer, Hinrich; Neumann, Thomas; Osadczuk, Andrzej; Janke, Wolfgang; Puff, Thomas; Blanz, Thomas; Gingele, Franz Xaver; Dannenberger, Dirk; Witt, Gesine: Das Oderhaff. Beiträge zur Rekonstruktion der holozänen geologischen Entwicklung und anthropogenen Beeinflussung des Oder-Ästuars.

29 (1998) Matthäus, Wolfgang; Nausch, Günther; Lass, Hans Ulrich; Nagel, Klaus; Siegel, Herbert:
Hydrographisch-chemische Zustandseinschätzung der Ostsee 1997

30 (1998) Fennel, Katja:
Ein gekoppeltes, dreidimensionales Modell der Nährstoff- und Planktondynamik für die westliche Ostsee

31 (1998) Lemke, Wolfram:
Sedimentation und paläogeographische Entwicklung im westlichen Ostseeraum (Mecklenburger Bucht bis Arkonabecken) vom Ende der Weichselvereisung bis zur Litorinatransgression

32 (1998) Wasmund, Norbert; Alheit, Jürgen; Pollehne, Falk; Siegel, Herbert; Zettler, Michael L.:
Ergebnisse des Biologischen Monitorings der Ostsee im Jahre 1997 im Vergleich mit bisherigen Untersuchungen

33 (1998) Mohrholz, Volker:
Transport- und Vermischungsprozesse in der Pommerschen Bucht

34 (1998) Emeis, Kay-Christian; Struck, Ulrich (Editors):
Gotland Basin Experiment (GOBEX) - Status Report on Investigations concerning Benthic Processes, Sediment Formation and Accumulation

35 (1999) Matthäus, Wolfgang; Nausch, Günther; Lass, Hans Ulrich; Nagel, Klaus; Siegel, Herbert:
Hydrographisch-chemische Zustandseinschätzung der Ostsee 1998

36 (1999) Schernewski, Gerald:
Der Stoffhaushalt von Seen: Bedeutung zeitlicher Variabilität und räumlicher Heterogenität von Prozessen sowie des Betrachtungsmaßstabs - eine Analyse am Beispiel eines eutrophen, geschichteten Sees im Einzugsgebiet der Ostsee (Belauer See, Schleswig-Holstein)

37 (1999) Wasmund, Norbert; Alheit, Jürgen; Pollehne, Falk; Siegel, Herbert, Zettler, Michael L.:
Der biologische Zustand der Ostsee im Jahre 1998 auf der Basis von Phytoplankton-, Zooplankton- und Zoobenthosuntersuchungen

38 (2000) Wasmund, Norbert; Nausch, Günther; Postel, Lutz; Witek, Zbigniew; Zalewski, Mariusz; Gromisz, Sławomira; Łysiak-Pastuszak, Elżbieta; Olenina, Irina; Kavolyte, Rima; Jasinskaite, Aldona; Müller-Karulis, Bärbel; Ikauniece, Anda; Andrushaitis, Andris; Ojaveer, Henn; Kallaste, Kalle; Jaanus, Andres:
Trophic status of coastal and open areas of the south-eastern Baltic Sea based on nutrient and phytoplankton data from 1993 - 1997

39 (2000) Matthäus, Wolfgang; Nausch, Günther; Lass, Hans Ulrich; Nagel, Klaus; Siegel, Herbert:
Hydrographisch-chemische Zustandseinschätzung der Ostsee 1999

40 (2000) Schmidt, Martin; Mohrholz, Volker; Schmidt, Thomas; John, H.-Christian; Weinreben, Stefan; Diesterheft, Henry; Iita, Aina; Filipe, Vianda; Sangolay, Bomba-Bazik; Kreiner, Anja; Hashoongo, Victor; da Silva Neto, Domingos:
Data report of R/V "Poseidon" cruise 250 ANDEX'1999

41 (2000) v. Bodungen, Bodo; Dannowski, Ralf; Erbguth, Wilfried; Humborg, Christoph; Mahlburg, Stefan; Müller, Chris; Quast, Joachim; Rudolph, K.-U.; Schernewski, Gerald; Steidl, Jörg; Wallbaum, Volker:
Oder Basin - Baltic Sea Interactions (OBBSI): Endbericht

42 (2000) Zettler, Michael L.; Bönsch, Regine; Gosselck, Fritz:
Verbreitung des Makrozoobenthos in der Mecklenburger Bucht (südliche Ostsee) - rezent und im historischen Vergleich

43 (2000)   Wasmund, Norbert; Alheit, Jürgen; Pollehne, Falk; Siegel, Herbert:
Der biologische Zustand der Ostsee im Jahre 1999 auf der Basis von Phytoplankton- und Zooplanktonuntersuchungen

44 (2001)   Eichner, Christiane:
Mikrobielle Modifikation der Isotopensignatur des Stickstoffs in marinem partikulären Material

45 (2001)   Matthäus, Wolfgang; Nausch, Günther (Editors):
The hydrographic-hydrochemical state of the western and central Baltic Sea in 1999/2000 and during the 1990s

46 (2001)   Wasmund, Norbert; Pollehne, Falk; Postel, Lutz; Siegel, Herbert; Zettler, Michael L.:
Biologische Zustandseinschätzung der Ostsee im Jahre 2000

47 (2001)   Lass, Hans Ulrich; Mohrholz, Volker; Nausch, Günther; Pohl, Christa; Postel, Lutz; Rüß, Dietmar; Schmidt, Martin; da Silva, Antonio; Wasmund, Norbert:
Data report of R/V "Meteor" cruise 48/3 ANBEN'2000

48 (2001)   Schöner, Anne Charlotte:
Alkenone in Ostseesedimenten, -schwebstoffen und -algen: Indikatoren für das Paläomilieu?

49 (2002)   Nausch, Günther; Feistel, Rainer; Lass, Hans Ulrich; Nagel, Klaus; Siegel, Herbert:
Hydrographisch-chemische Zustandseinschätzung der Ostsee 2001
Pohl, Christa; Hennings, Ursula:
Ostsee-Monitoring - Die Schwermetall-Situation in der Ostsee im Jahre 2001

50 (2002)   Manasreh, Riyad:
The general circulation and water masses characteristics in the Gulf of Aqaba and northern Red Sea

51 (2002)   Wasmund, Norbert; Pollehne, Falk; Postel, Lutz; Siegel, Herbert; Zettler, Michael L.:
Biologische Zustandseinschätzung der Ostsee im Jahre 2001

52 (2002)   Reißmann, Jan Hinrich:
Integrale Eigenschaften von mesoskaligen Wirbelstrukturen in den tiefen Becken der Ostsee

53 (2002)   Badewien, Thomas H.:
Horizontaler und vertikaler Sauerstoffaustausch in der Ostsee

54 (2003)   Fennel, Wolfgang; Hentzsch, Barbara (Herausgeber):
Festschrift zum 65. Geburtstag von Wolfgang Matthäus

55 (2003)   Nausch, Günther; Feistel, Rainer; Lass, Hans Ulrich; Nagel, Klaus; Siegel, Herbert:
Hydrographisch-chemische Zustandseinschätzung der Ostsee 2002
Pohl, Christa; Hennings, Ursula:
Die Schwermetall-Situation in der Ostsee im Jahre 2002

56 (2003)   Wasmund, Norbert; Pollehne, Falk; Postel, Lutz; Siegel, Herbert; Zettler, Michael L.:
Biologische Zustandseinschätzung der Ostsee im Jahre 2002

57 (2004)   Schernewski, Gerald; Dolch, Tobias (Editors):
The Oder estuary against the background of the European Water Framework Directive

58 (2004)   Feistel, Rainer; Nausch, Günther; Matthäus, Wolfgang; Łysiak-Pastuszak, Elżbieta; Seifert, Torsten; Sehested Hansen, Ian; Mohrholz, Volker; Krüger, Siegfried; Buch, Erik; Hagen, Eberhard:
Background Data to the Exceptionally Warm Inflow into the Baltic Sea in late Summer of 2002

59 (2004)   Nausch, Günther; Feistel, Rainer; Lass, Hans Ulrich; Nagel, Klaus; Siegel, Herbert:

Hydrographisch-chemische Zustandseinschätzung der Ostsee 2003

Pohl, Christa; Hennings, Ursula:

Die Schwermetall-Situation in der Ostsee im Jahre 2003

60 (2004)   Wasmund, Norbert; Pollehne, Falk; Postel, Lutz; Siegel, Herbert; Zettler, Michael L.:

Biologische Zustandseinschätzung der Ostsee im Jahre 2003

61 (2004)   Petry, Carolin:

Mikrobieller Abbau von partikulärem organischen Material in der tiefen Wassersäule

62 (2005)   Nausch, Günther; Feistel, Rainer; Lass, Hans Ulrich; Nagel, Klaus; Siegel, Herbert:

Hydrographisch-chemische Zustandseinschätzung der Ostsee 2004

Pohl, Christa; Hennings, Ursula:

Die Schwermetall-Situation in der Ostsee im Jahre 2004

63 (2005)   Umlauf, Lars; Burchard, Hans; Bolding, Karsten:

GOTM – Scientific Documentation. Version 3.2

64 (2005)   Wasmund, Norbert; Pollehne, Falk; Postel, Lutz; Siegel, Herbert; Zettler, Michael L.:

Biologische Zustandseinschätzung der Ostsee im Jahre 2004

65 (2006)   Matthäus, Wolfgang:

The history of investigation of salt water inflows into the Baltic Sea - from the early beginning to recent results

66 (2006)   Nausch, Günther; Feistel, Rainer; Lass, Hans Ulrich; Nagel, Klaus; Siegel, Herbert:

Hydrographisch-chemische Zustandseinschätzung der Ostsee 2005

Pohl, Christa; Hennings, Ursula:

Die Schwermetall-Situation in der Ostsee im Jahre 2005

67 (2006)   Rößler, Doreen:

Reconstruction of the Littorina Transgression in the Western Baltic Sea

68 (2006)   Yakushev, Evgeniy V.; Pollehne, Falk; Jost, Günter; Kuznetsov, Ivan; Schneider, Bernd; Umlauf, Lars:

Redox Layer Model (ROLM): a tool for analysis of the water column oxic/anoxic interface processes